www.usn.no

FMH606 Master's Thesis 2023
Electrical Power Engineering

Modeling of hot-spots in transformer using analytical or numerical methods

<optional figure>

Muhammad Muneeb

Faculty of Technology, Natural Sciences and Maritime Sciences
Campus Porsgrunn

www.usn.no

Course:	FMH606 Master's Thesis 2023
Title:	*Modeling of hot-spots in transformer using analytical or numerical methods*
Pages:	*113*
Keywords:	*Transformer, Thermal model, Hotspot, COMSOL Multiphysics®*

Student:	*Muhammad Muneeb*
Supervisor:	*Thomas Øyvang, Dany Tome, Frederic Maurer*
External partner:	*Skagerak Kraft, SysOpt Project, Hitachi Energy*

Summary:

Due to the increasing penetration of renewable energy sources into electrical grids, high variation of power becomes a problem for the stability of power systems. To keep the system balanced, hydro generators occasionally operate in boosting mode during short time intervals, which produces more reactive power than the threshold ($Q > 1 p.u.$). This leads to Transformer and Excitation systems operating at higher ratings which results in thermal stress.

The main goal of this thesis is to analyze the thermal impact on the transformers when operated in boosting mode. Two main approaches are performed in this thesis, simple analytical modeling in *Julia* and numerical modeling of electromagnetics and thermodynamics in *Comsol Multiphysics®* of transformers are studied.

The model for the 2D-numerical modeling is a $5MVA$ air-cooled three-phase distribution transformer which is located in Uleberg and owned by Agder Energy. Magnetic flux density in the core, current density, heat loss density, and temperature are discussed in the results. Effects of change in Ambient temperature and cooling conditions are also inspected in the results.

Preface

This master's thesis was the final task of Electrical Power Engineering at the University of South-Eastern Norway (USN). The thesis was conducted from January to mid-May during the spring semester of 2023 and based on 30 ECTS.

This thesis was conducted under the supervision of associate professor Thomas Øyvang at USN, with guidance from co-supervisors Frédéric Maurer from NTNU and Dany Josue Tome Robles, stipendiat at USN. We did virtual meetings almost every week. It's my honor to express my gratitude to all those people who supported and motivated me throughout this work. Firstly, my sincere gratitude goes to my main supervisor Thomas Øyvang for sharing his knowledge about transformers, and arranging data despite some challenges. He arranged data from Skagerak and meetings with Prof. Gunne John Hegglid for guidance, and hours of discussions. He helped me to access *Comsol* and run simulations throughout the thesis. Thanks to my co-supervisor Frédéric Maurer for hosting weekly meetings even in his very busy routine and guiding me the right way, especially for numerical modeling. Special thanks to my co-supervisor Dany Josue Tome Robles, who give me extra time besides scheduled meetings and guided me in learning *Comsol* at the start. He also helped in analytical thermal modeling in *Julia* and shared his precious knowledge about neural networks too. Thanks to the IT team of USN for helping me with the license of the *Comsol* modules. I am very thankful to *Hitachi Energy* and *Skagerak Energi* for giving access to transformers data for this project.

Finally, a very special thanks and sincere gratitude to my family. My grandfather, parents, and siblings for their prayers, and best wishes throughout the work. Thanks to my sister, Rimsha Perveen from the University of Engineering and Technology, who helped me with theoretical knowledge and proofreading of this thesis. My final gratitude goes to my classmates who somehow made my two years of online and hybrid time memorable and enjoyable in their good company.

Porsgrunn, 15th May 2023

Muhammad Muneeb

Contents

List of Figures

List of Tables

Nomenclature

Symbol	Explanation
CB	Circuit Breaker
LV	Low Voltage
HV	High Voltage
FEM	Finite Element Method
OFWF	Oil Forced Water Forced
ONAN	Oil Natural Air Natural
OA	Oil Immersed self cooled
FBG	Fiber Bragg Grating
CSV	Comma Separate Values
RC	Resistor Capacitor
RMS	Root Mean Square
AC	Alternating Current
emf	Electromotive force
DC	Direct Current
ECTS	European Credit Transfer and Accumulation System

1 Introduction

1.1 Background

Electric energy has a significant contribution to our day-to-day existence by effectively delivering energy to the users. The power system ensures the generation of electric energy from other forms of energy e.g., hydropower, and transmitting to the consumers.

Electric Supply is mainly divided into three categories, generation, transmission, and distribution. Power systems consist of many critical components e.g., transformers, circuit breakers (CB), switch gears, cables, etc., and their combination helps in successful power delivery to customers [1].

Power transformers are playing a vital role in the transmission and distribution of electricity, and they are considered the largest investment in the power transmission category. Outages of power transformers are highly undesirable and cause considerable loss to the economy of electrical networks [2].

A power transformer is a static device that at least has two windings, primary and secondary. Two sides are connected with electromagnetic induction, transforming one set of voltage and current into another set of voltage and current while keeping the frequency constant, according to the requirement to minimize losses [3].

When defining transformer ratings, the temperature of hot spots of the windings is one of the evaluation parameters in assigning thermal and overloading capacity.

1.2 Motivation

Since the population of the world is increasing, hence the demand for electricity is increasing accordingly. To cope with the high demand, more electricity sources are considered that are clean and cost-effective which are called renewable energy sources. Common renewable energy sources are water, solar, wind, etc. An increase in this energy will help in transitioning towards a more prosperous, green, and independent economy. Europe has passed the goal of 20% of total energy coming from renewable sources by the end of

2020, now its 22%, and the target to achieve climate neutrality by the end of 2050 for clean affordable energy [4].

Merging this into existing grids has several challenges due to its varying nature. Solar energy, for instance, depends on the sunlight, the capacity of solar power plants will be affected in the presence of clouds. Wind power plants depend on wind, which is not constant throughout the day/seasons, sudden increases in demands of power cannot be entertained. In short, this causes more voltage fluctuations and unbalanced loading. This required reactive power management in the grid to improve voltage fluctuations and stability. Synchronous generators can generate reactive powers in the grid when they are operated in boosting mode to balance the grid. The duration of boosting mode can be from several minutes to a few hours depending on achieving equilibrium. Transformers are one of the top investments in equipment and they must be able to handle that extra thermal stress due to the boosting mode, without damaging their insulation and coils. This thesis analyses the thermal modeling of transformers and magnetic flux density, heat loss density, and resistive loss, to ensure transformer security and uninterrupted power supply without load shedding.

1.3 Problem statement

In recent years, enormous progress has been observed in merging renewable energy generators (REGs) with the existing power grid. In 2021, 21% of the total power generation in Europe was from renewable sources while targets are to reach 40% by the end of 2023 [4]. From 2020 to 2021, Norway increases 3.07% power generation from renewable sources, figure 1.1 compares the increase of energy from renewable sources in one year (2020 - 2021).

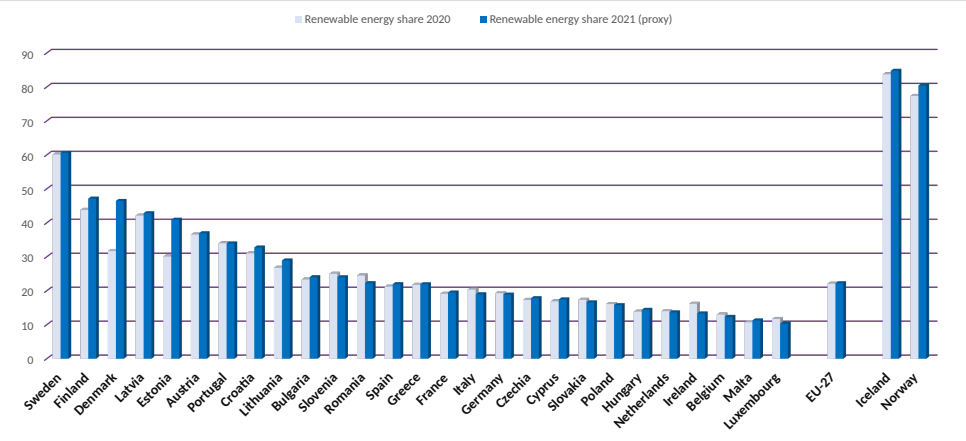

Figure 1.1: Share of energy from renewable sources [4]

This has a strong impact on the reactive power, which results in issues related to steady-state voltages and causes transient/stability issues. Hydro generators are often required to operate beyond the limits for limited time periods. This is called the boosting mode of generators when they are producing much more reactive power (Q > 1 p.u.) to ensure grid stability.

Transformers are one of the most expensive components of the power grids, therefore it is of utmost importance to analyze the limits of transformers if they can withstand the thermal stresses during the boosting operating mode and continue uninterrupted power supply to consumers. In this thesis, transformer electromagnetic and thermal behavior is discussed in detail with different operating conditions with varying cooling situations to analyze if the transformer can withstand overloading during boosting mode.

- Analyze three-phase 2D-Finite Element Method (FEM) main transformer.
- Analyze the cooling methods and their effects on the temperature of the transformer.
- Literature review of used thermal loss models.
- Building an Analytical model and comparing it with a transformer from the *Skagerak Energi*.
- Computing the temperature rise of the FEM model.

1.4 Outline of the thesis

The approach used in this thesis starts with the precise introduction of transformers and their types which follows the thermal analytical modeling of $118MVA$ OFWF transformer from the *Skagerak Energi*. The primary focus of this thesis is on the electromagnetic and thermal modeling of the $5MVA$ dry-type, air-cooled, three-phase distribution transformer which is located at Uleberg and owned by Agder Energy. A simulation model of this transformer was built in COMSOL Multiphysics®, which will do FEM analysis by combining multiple physics including electromagnetics, heat transfer, electrical circuits, and laminar flow. Some adjustments are made to improve the modeling in material properties and solver settings while the rest of the settings stayed default. Discussions and future work is presented in the closing chapters of this thesis. Data is processed in *MATLAB* and *Excel* while analytical modeling is based on *Julia* in Jupiter's notebook. The appendix C contains relevant neural network coding used for parameter estimation in *Julia*.

2 Theory

This section is based on a brief introduction to the basic concepts. These details of the equations used in numerical modeling will be discussed in chapter 4 later.

2.1 Introduction to Transformers

Transformers are used to step up the voltage to minimize losses during transmission over long distances and later step down according to the requirement of residential and commercial loads. Transformers are commonly classified as dry type and oil filled. Dry-type transformers do not use oil as coolant and hence they are preferred in places where the risk of fire hazard must be kept low [5].

Since dry-type transformers use only air instead of oil for cooling, hence the temperature of these transformers goes higher than oil filled. The life of the transformer is highly dependent on the temperature rise therefore it is necessary to build a model to calculate the expected temperature rise. In 1944, Stewart and Whitman presented one of the earliest methods for temperature prediction [6]. With the advancement of computers, it became easier to get more accurate results using numerical approximation.

It is essential to estimate the correct lifetime of the transformer and overloading capabilities to keep running uninterrupted power supply. Strain is among the several significant factors that affect the lifetime of transformers which is further classified as thermal, electrical, and mechanical stresses [7].

2.1.1 Dry-type Transformer

In Dry-type transformers, winding does not contain insulating material nor core is dipped into any liquid rather, the windings core is located inside the sealed tank which is pressurized with air as shown in Figure 2.1 [8], [9]. Dry-type transformers are of two types, Cast Resin, and Vacuum pressure impregnated. Cast Resign type transformer is preferred in those areas where moisture content is very high in the atmosphere because both sides of windings are encapsulated with epoxy resin. This encapsulation prevents moisture contact with windings and hence transformer is nonabsorbent to moisture. These transformers

are available in the rating from $25kVA$ to 12500 kVA. Some of the benefits of this type of transformer are, better overloading capacity, high efficiency due to low partial discharges, and zero risk of fire hazard because of non-inflammable winding insulation [8].

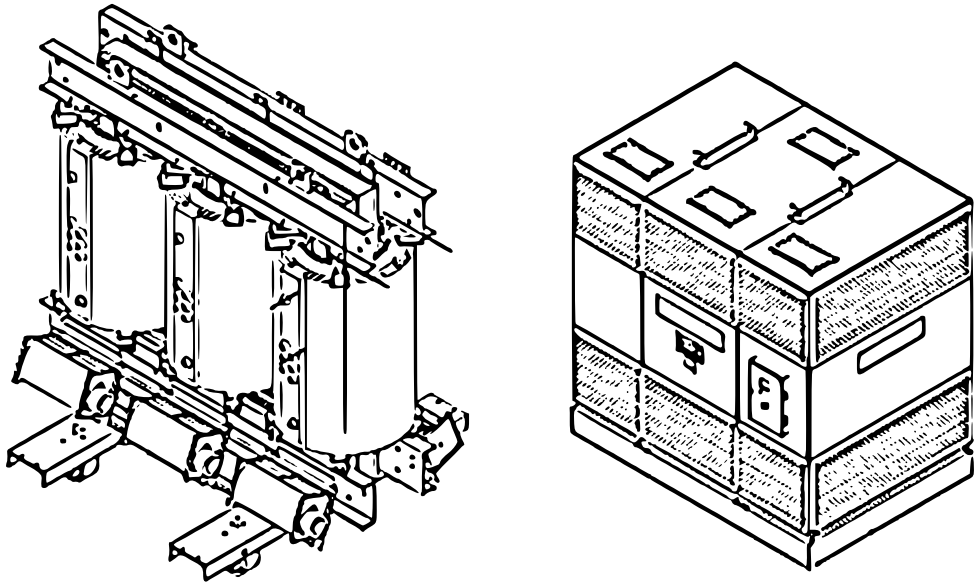

Figure 2.1: Dry type transformer and enclosure [9]

The material used for insulation of a Vacuum Pressure impregnated transformer is a minimum flammable material. Depending on the voltage levels, windings of this type of transformer are made in the form of foils, continuous strips, and disks. This is available from $5kVA$ to 30 MVA. Some advantages of using this type of transformer include Void free insulation, fewer temperature fluctuations and fewer chances for fire [8]. The lifetime of the transformers depends on the temperature rise of the hot spots during overloading, which is discussed in the coming sections.

2.1.2 Oil Immersed Transformer

The oil-immersed transformers use oil to minimize the transformer's temperature. They are also named oil-filled transformers. The body of the oil-immersed transformer is placed in a welded steel oil tank that is filled with insulating oil as shown in figure 2.2. When oil filled transformer operates, the heat from the core and the coils is first transferred into the insulation oil and then to the cooling medium. Since this type of transformer has oil-immersed coils so it lowers the heat map of the devices enclosed by it [10].

The oil-immersed transformers consist of three basic parts magnetic core, windings, and bushings. The magnetic core produces the path for magnetic flow. The windings consist

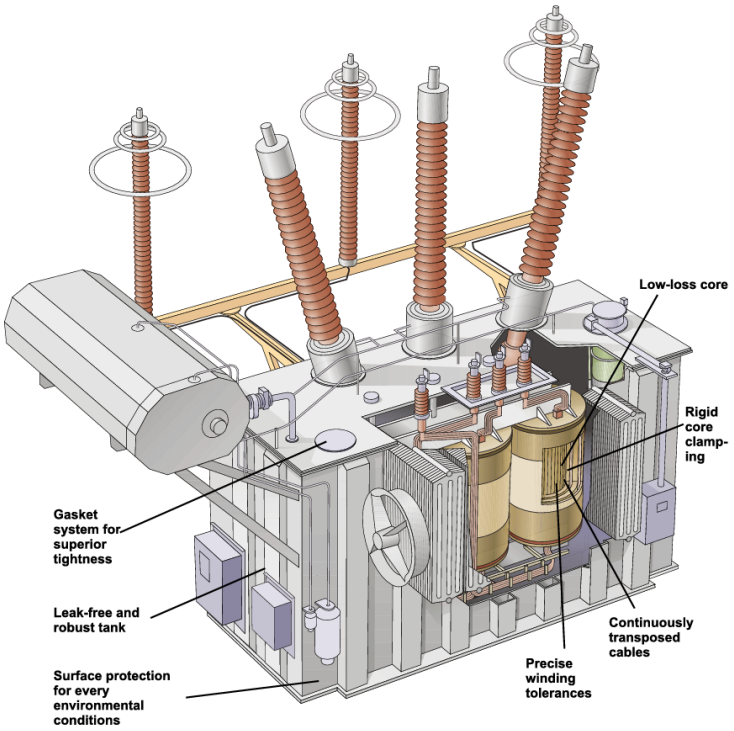

Figure 2.2: Oil immersed transformer [11]

of a conductor coil that is wrapped around the core and is used to produce a magnetic field. Bushings are used to connect the transformer windings to the substation [10].

This type of transformer is used in electrical substations or in power distribution. The standard rating of oil-immersed transformers is below 200 kVA. However, expectations are to be made for situations where high voltage is needed [12]. Oil-immersed transformers have several characteristics as follows, it has good heat dissipation, large capacity, and fewer losses [13].

The primary function of the distribution oil-immersed transformer is to transform high voltages to lower voltages so that it can be used for the housed hold or commercial purposes. It reduces the voltage rating by using the principle of induction or Faraday's law. Common rating oil immersed transformers that distribute electricity for small industrial requirements is $33kV$ while for residential use it provides $440\,V$ and $220\,V$ [12].

2.1.3 Core-type construction

The core of three phase transformer consists of three limbs and each leg of the core carries primary and secondary windings. Each leg of the core has at least one high-voltage winding (HV) and one low-voltage winding (LV). Proper insulation is applied to

the core to minimize eddy current losses. As the name shows, low-voltage windings have less voltage, so lamination is applied to this side because it is easier. The low voltage winding is close to the core while high voltage winding is placed above low voltage winding with proper insulation. In this type of construction, windings are linked magnetically with one another [14].

2.1.4 Shell-type construction

Three phases shell type transformer is usually set up by three individual single-phase transformers. These types of transformers are independent as compared to the three-phase core type transformers [14]. High and low voltage windings are present around the three main limbs and like the core type construction transformer the low voltage windings are close to the core [15]. In these transformers flux that is produced by the windings is in phase as the magnetic circuits are parallel to each other. The voltage waveform of shell-type transformers is less distorted, which is why shell-type transformers are preferred [14].

Five limb core is used in the transformers that have larger power. The height of these five limb core type transformers is lower and their stray fluxes and eddy current losses are also less [16].

2.2 Structure of the Transformer

A power transformer has the following main components [16] [17] :

- Core
- Tank
- Windings
- Taps
- Insulation systems
- Cooling Systems
- Protective equipage
- Other structural components

Commonly a power transformer has two or more concentric separate windings that are wound around the soft iron limb or the core for each phase that provides the necessary magnetic circuit [16]. The core, tank, windings, insulation, and cooling systems play a vital role in electromagnetic induction, so these will be discussed in upcoming sections.

2.2.1 Core

The magnetic circuit of the transformer is called the core which is designed to provide a path for magnetic field flow. It has two windings entitled primary and secondary windings. When AC current passes through a primary winding, due to the principle of Faraday's law of electromagnetic induction (Magnetic field (flux) is created when current is passed through a coiled wire) magnetic flux is produced and as a result, emf is induced in secondary windings [18].

There are two types of construction for cores, core type, and shell type. In shell-type construction the core is around the coil therefore the magnetic fields are around the outside of the coil. In core-type construction, the coils are wound outside of the core [19]. Core type construction is most widely used in transformers due to simple design, Core type construction for single phase transformers is shown in (a) while shell type is in (b) of Figure 2.3.

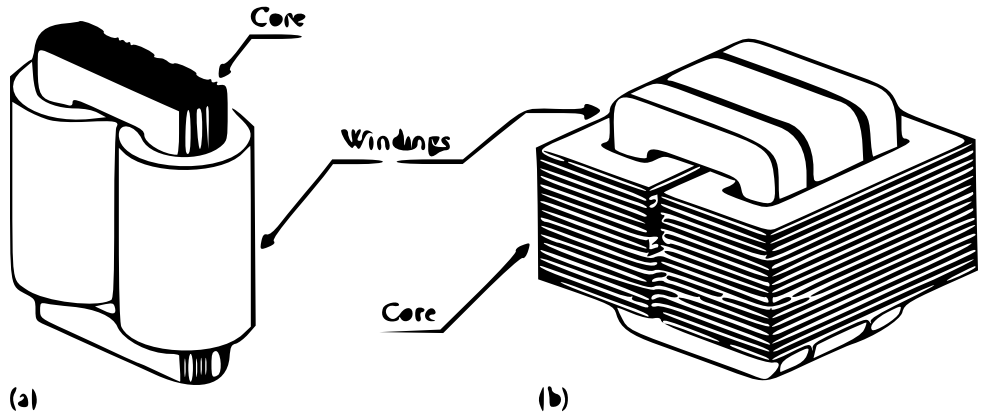

Figure 2.3: Core type core and shell type core (b) [20].

Whenever high power or high voltage is needed core type transformers are used although their power losses are higher. The windings of the core-type transformers are readily available, so their maintenance is easier as compared to the shell-type transformers. Since in core-type transformers, the windings are on separate legs so more copper is required for the manufacturing of core-type transformers. On the other hand, shell-type core construction is used for lower-power applications. However, their energy losses are lower, but maintenance is harder. The mechanical strength of shell-type transformers is also higher as compared to that of core-type transformers [21].

A core is an integral part of the power transformer. To carry the linkage flux through the windings it generates a close magnetic circuit with low reluctance. The quality of the core plays a vital role in the performance of transformers. There are several factors that constitute the quality of the core that includes magnetization current, no-load losses, and volts per turn [17].

The core is stacked by thin lamination of electrical sheets having a thickness of about 0.3mm or less, that are coated with a thin layer of insulation material having a thickness of about 10-20 µm that prevents large eddy current paths in the core [22].

The choice between these cores is made on the basis of required power and height limits with regard to transportation. A three-phase transformer is used whenever a higher power transfer is required. In three-phase transformers, there are two types of cores three limbs (core-type construction) and five limbs (shell-type construction). In these types of cores, there are three limbs that are surrounded by windings.

2.2.2 Tank

The tank of the transformer is a closed structure that is made of steel plates having a thickness of about a few centimeters. A transformer tank is also called a transformer tank body. It is made up of steel plates having a closed structure. It has several functions as it holds and protects the windings, core, and dielectric fluid inside it. To reduce the deflection and the stresses in the plates while loading, stiffeners are provided on all the sides of the transformer tank [17].

The tanks are designed in such a way that they can bear higher pressure than the operating pressure as is also specified by the relevant guidelines because it has to bear several types of loads such as vacuum and pressure loads besides jacking, lifting, etc [17]. It must hold out against the forces imposed on it during transportation. Another important consideration made while designing a tank is its cover should be removable so that it can provide access for the installation, inspection, and removal purposes of core and windings, bushing connections winding temperature, off-circuit tapping links, etc. (if required). As manufacturers have to access these items and parameters to ensure the proper working of transformers. The cover is normally just a stiffened flat plate. While designing the tanks they must be provided with valves for filling and drainage and to allow the oil samples to be taken for analysis whenever it is required [17], [22].

2.2.3 Windings

The windings are generally made of high-quality of copper. The transformer windings consist of a set of several radial (horizontal) channels that separate the discs of copper wires from one another. With the help of these horizontal channels, a connection is made

between the inner and outer vertical channels [23]. To avoid the connection between each turn of the winding, insulation is provided with an enamel coating. There are two types of windings used in the transformers, primary windings, and secondary windings. The winding that receives the electrical energy is called the primary windings and the winding that transmits the electrical energy to the load is called the secondary windings [24]. Windings are capable of increasing or decreasing the current or voltage level.

2.2.4 Taps

Transformer taps are used to alter the turn ratio. It is basically a voltage regulation method as by changing the number of turns in one winding of the transformer the voltage can be varied as voltage depends on the turn ratio [25]. The basic principle of a tap changer is shown in figure 2.4. Many transformers have these taps either on primary windings or secondary windings to change the turn ratio to maintain the voltage to the desired level [18]. Taps are also used to control the active power and the reactive power [25]. For some of the transformer's taps can be changed under the loading condition while for other transformers they must be de-energized [18].

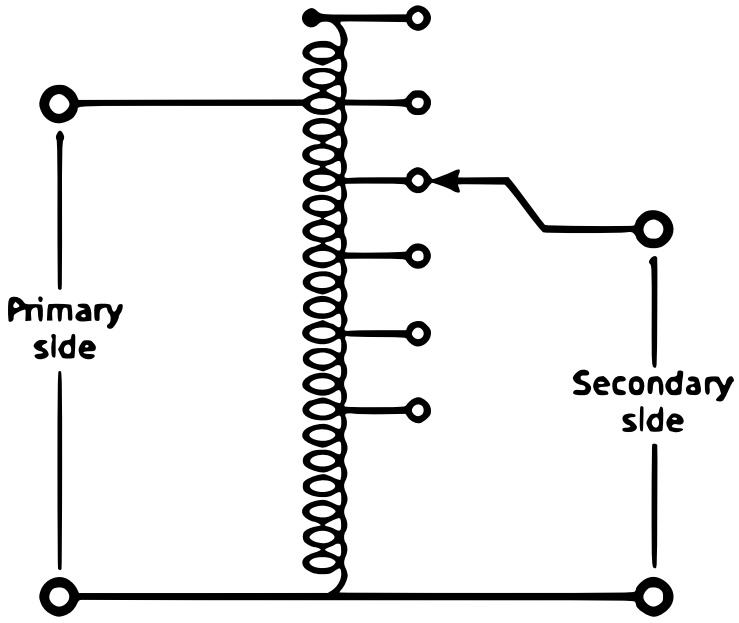

Figure 2.4: Tap changing principle [25].

2.2.5 Insulation systems

Like many other electrical devices transformers also produce heat in the form of losses during their operation and this heat then increases the temperature of the transformers.

This higher temperature can cause serious problems, so this is a big challenge for design engineers to design a product that is reliable and has efficient performance. That's where the insulation system comes in to keep the transformer temperature within acceptable limits. The life of the transformer is highly dependent on the temperature limits because over-temperature damages the insulation and causes a reduction of average life [26]. Insulation is divided into classes (thermal) for the transformers, generators, and motors. Insulation classes B, F, and H are among the widely used classes, these are classified according to the operating temperatures.

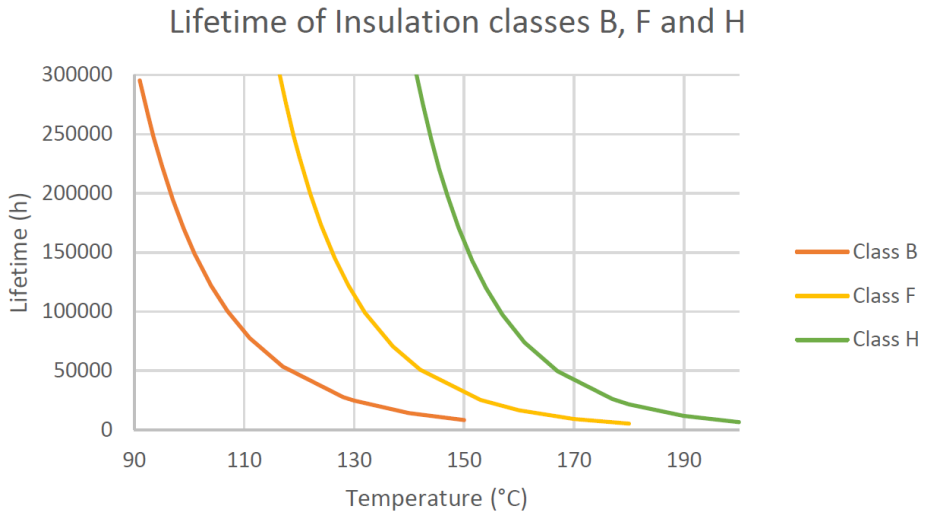

Figure 2.5: Insulation classes lifetime against temperature increase [5]

Figure 2.5, shows the average lifetime of class B, F, H vs the increase in temperature. The plot shows the decrease in a lifetime from 300000 hours (34 years) to 0 hours with the increase in temperature. According to the general rule of thumb, there is a decrease of 10 $^{\circ}C$ increase in operating temperature, reducing the lifetime to half [5].

2.2.6 Cooling systems

Since no transformer is ideal, they produce heat due to different losses, therefore cooling mechanism must be adopted to properly operate transformers. Methods of cooling depend on the application, size, and amount of heat needed to dissipate [27].

The oil used in the transformers serves two purposes, first to behave as an insulator and second, it transports heat from the transformer to outside. It is important that the transformer must have proper cooling ducts and circulating paths around the heat source so that the cooling medium efficiently removes the heat. The natural circulation of oil through the transformer due to the convection is called the "thermosiphon" effect. The

heat is taken out through the insulating medium (circulating oil) to the tank from where it is transferred to the surrounding environment through tank walls. Radiators are used in the process to boost the rate of convection without increasing the size of the transformer tank. In some transformers, fins are also used to increase the surface area for cooling oil. Rate of the cooling depends on the rate of heat transfer from oil to the surrounding, fans are installed to increase this rate of heat dissipation. Larger transformers even use pumps for faster and proper circulation of oil and external heat exchanger for cooling the oil, external cooling medium can also be used e.g., air or water. For instance, the transformer located at Sundsbarm power plant used water as an external (secondary) coolant [27].

There are two types of fluid flow for cooling transformers. First, the natural convection, fluid flowing through the windings is called the non-directed flow while if the flow is guided with the help of fans and pumps, etc., this is referred to as directed flow. Directed flow has more control of the fluid flow through windings [27].

To increase the cooling, forced circulation is used where fans and pumps with secondary coolers are used. One of the benefits of forced cooling is that transformer can be used in the boosting mode or at higher ratings without increasing the size of the transformer. A transformer can have cooling stages, that increase transformer capacity to work at higher ratings and use supplementary cooling equipment only when needed at higher loads and hence efficiency increases [27].

Usually, transformer cooling class is expressed by four-letter coding which is given in table 2.1. This system of representation is an international standard where the first two letters are used to express the internal cooling system while the latter two letters are used to express the external cooling setup, even if external cooling is not included, the code letters still be four which was not the case in the United States where they were using two letters code before standardization. For instance. For example, OA was classified as oil immersed self-cooled in the United States but now it is replaced by ONAN which means Oil Natural, Air Natural [27].

Oil Forced Water Forced Cooling Method (OFWF)

The transformer used in this thesis has (OFWF) cooling system. This (OFWF) is generally used for very large transformers that have ratings higher than 100 MVA [28] and the transformer covered in this thesis for analytical modeling has a rating of 118 MVA. As the specific heat capacity of water is higher than atmospheric air that is why water is good heat exchanger media as compared to air. In the oil forced water forced cooling method hot oil is circulated with the help of a pump from the top of the transformer's tank to "oil to the water heat exchanger", where oil is then cooled with the help of water showers on the oil pipes of the heat exchanger. In this way, water is used to separate the heat from the oil. The cold oil is then pumped back to the bottom of the transformer's tank as shown in figure 2.6, [28], [29].

Table 2.1: Cooling classes in transformers [27].

Internal/External	Letter place	Code Letter	Description
Internal	First letter	O	Liquid with a flash point less than or equal to 300°C
Internal	First letter	K	Liquid with a flash point greater than 300°C.
Internal	First letter	L	Liquid with no measurable flash point
Internal	Second letter	N	Natural convection through cooling equipment and windings
Internal	Second letter	F	Forced circulation through cooling equipment, natural convection in windings
Internal	Second letter	D	Forced circulation through cooling equipment, directed flow in main windings
External	Third letter	A	Air
External	Third letter	W	Water
External	Fourth letter	A	Natural convection
External	Fourth letter	F	Forced convection

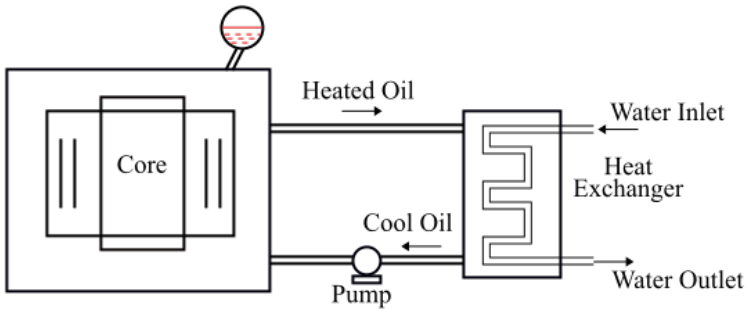

Figure 2.6: Oil Force Water Force cooling system [28]

2.2.7 Protective equipage

Transformers are expensive equipment and faults in transformers can result in disruption of electricity and economic losses therefore it is crucial to have protective equipment for sooth operation. Three main reasons for transformer internal faults are an increase in phase current, differential current, and gas formation due to fault arc. Disconnecting the faulty unit from the rest of the network is done with the help of protection. The most used protections are: Over current protection Differential protection Rate of pressure rise

protection The first protection during a fault is usually over current protection and it is almost available in every transformer even in smaller transformers as well. Differential relays are based on differential currents while the rate of pressure rise protection is for arcing faults.

2.3 Single phase vs three phase transformer

A transformer that has one pair of primary and secondary windings is called a single-phase transformer while a transformer that has three pairs of windings in a three-sectioned iron core and each section consisting of a pair of primary and secondary winding is called a three-phase transformer. The design of a single-phase transformer is simple while three-phase transformers have a complex design as they consist of three windings as shown in figure 2.7. The power handling capacity of single-phase transformers is less than three-phase transformers, which is why single-phase transformers are used for small loads like TVs, mobile chargers inverters, etc. Three-phase transformers are used where high power is required to run induction motors, they are also used in power systems for the distribution and transmission of power [30].

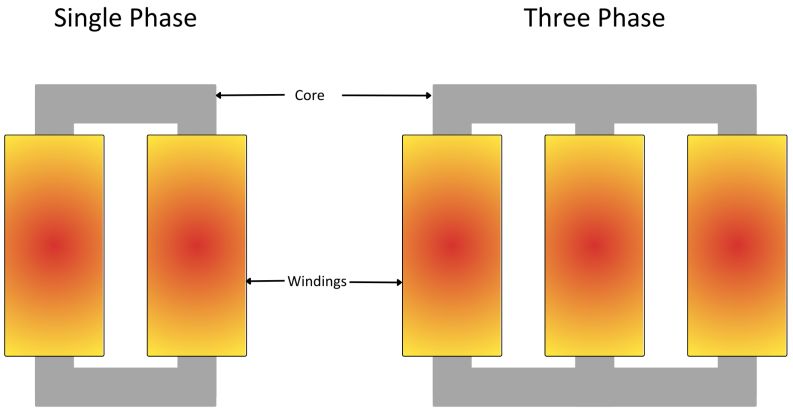

Figure 2.7: Single phase transformer vs three phase

There are two ways of providing three phase transformer system i.e., using three single-phase transformers or a single three-phase transformer. Single-phase three transformers are magnetically independent while in a three-phase transformer, there is a magnetic coupling between the phases. Every method had certain advantages over the other one. Three-phase transformers occupy less space, and they are more economical as it costs 15% less than three single-phase transformers. But sometimes transferring three-phase transformers to the site becomes very difficult. The main advantage of using three single-phase transformers is that if one of the transformers becomes out of order, then the

system can work because of the delta connection (as the system works on an open delta connection). Due to these reasons, three single-phase transformers are preferred for higher power and higher voltage units [16].

2.4 Turn ratio

The simplest single-phase transformer with two coils is shown in figure 2.8, where a rectangular shape core is used, with primary winding having N_p number of turns on one leg of the core while secondary windings with N_s turns are wounded on the other leg.

In the ideal transformer, the relationship between primary and secondary voltage is given by the turn ratio a between primary and secondary windings [5].

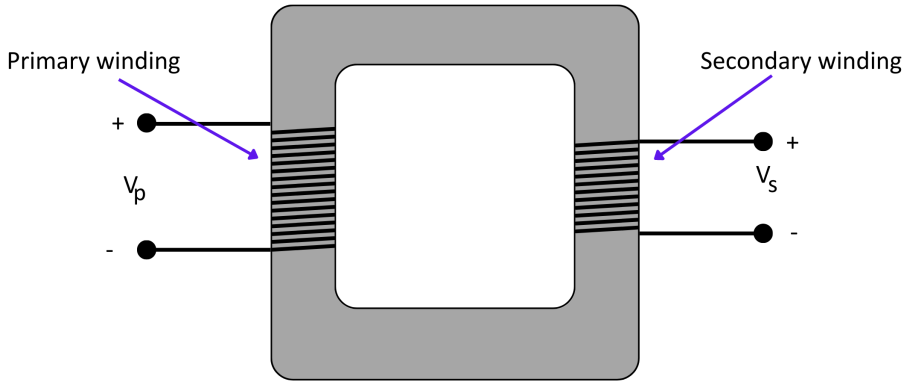

Figure 2.8: Single phase transformer windings

$$a = \frac{V_p}{V_s} = \frac{N_p}{N_s} \tag{2.1}$$

where,
N_p = number of turns in primary,
N_s = number of turns in secondary,
V_p = primary voltage,
V_s = secondary voltage.

Turn ratio a in equation 2.1 is valid when both primary and secondary windings have the same connections e.g., both start or both delta, otherwise phase difference needs to be considered and must be in phase.

The number of turns in a transformer depends on several factors such as the geometry of the transformer A_{core}, Alternating Current (AC) frequency f, the maximum flux density of the core A_{core}, and Root Mean Square Voltage V_{RMS}. Relationship between these qualities can be expressed as [6]:

$$N = \frac{\sqrt{2} \cdot V_{RMS}}{2\pi \cdot B_{max} \cdot A_{core} \cdot f} \tag{2.2}$$

Equation 2.2 is derived from Faraday's law of electromagnetism and detailed derivation can be found in Appendix A. This equation is based on the ideal scenario and assumed that there is no flux leaked.

2.5 Equivalent circuit

The equivalent circuit of a real transformer is shown in figure 2.9 which includes operational losses in a real scenario. The copper losses are the simplest to model and are represented by resistive losses, R_p in primary and R_s in secondary windings respectively. The power losses in the core are represented by a resistor R_c which consists of hysteresis and eddy current losses which are explained in a separate section of losses in this thesis. The reactance X_M is used to represent the excitation of the core (the magnetization current) [31].

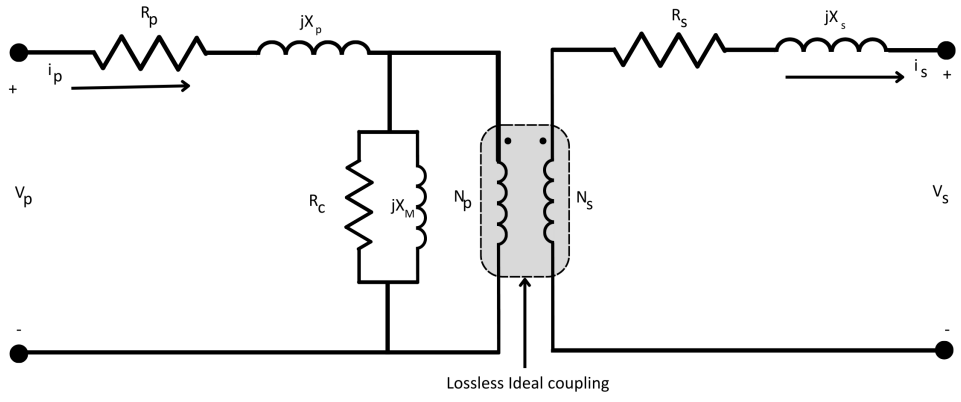

Figure 2.9: Equivalent circuit of a transformer

The induced voltages e_{Lp}, e_{Ls} due to leakage fluxes ϕ_{Lp}, ϕ_{Ls} in the primary and secondary windings can be expressed as equation 2.3 and equation 2.4 [31]:

$$e_{Lp} = N_p \frac{d\phi_{Lp}}{dt} \tag{2.3}$$

$$e_{Ls} = N_p \frac{d\phi_{Ls}}{dt} \tag{2.4}$$

The induced magnetic flux from the windings is not fully conducted through the core because some of it leaked out into the air. The reluctance $\mathfrak{R}$ of the air is constant and much larger than the core reluctance [31]. The leakage flux is directly proportional to the circuit current in the windings.

$$\phi_{Lp} = \frac{N_p}{\mathfrak{R}} \cdot i_p \tag{2.5}$$

$$\phi_{Ls} = \frac{N_p}{\mathfrak{R}} \cdot i_s \tag{2.6}$$

Substituting equations 2.5, 2.6 into equations 2.3 and 2.4 results:

$$e_{Lp} = N_p \frac{d}{dt}(\frac{N_p}{\mathfrak{R}}) \cdot i_p = \frac{N_p^2}{\mathfrak{R}} \cdot \frac{di_p}{dt} \tag{2.7}$$

$$e_{Ls} = N_s \frac{d}{dt}(\frac{N_s}{\mathfrak{R}}) \cdot i_s = \frac{N_s^2}{\mathfrak{R}} \cdot \frac{di_s}{dt} \tag{2.8}$$

The constants in the equations 2.7, 2.8 can be lumped together, and the resulting induced voltages e_{Lp}, e_{Ls} can be written as:

$$e_{Lp} = L_p \frac{di_p}{dt} \tag{2.9}$$

$$e_{Ls} = L_s \frac{di_s}{dt} \tag{2.10}$$

where $L_p = \frac{N_p}{\mathfrak{R}}$ and $L_s = \frac{N_s}{\mathfrak{R}}$ are the leakage inductance in primary and secondary windings respectively. Therefore, the leakage flux can be modeled by primary and secondary inductors while the reactance of the primary and secondary windings is represented by $X_p = 2\pi f L_p$ and $X_s = 2\pi f L_s$ respectively [31].

To analyze practical circuits of transformers it is common practice to simplify the circuit shown in figure 2.9 and convert it to an equivalent circuit with a single voltage level.

The equivalent circuit must be referred to either the primary or secondary side in the problem solution, in figure 2.10, it is drawn as a circuit that is referring to its primary side, where:

$R_{eq:p} = P_p + P_s a^2$,
$X_{eq:p} = X_p + X_s a^2$.

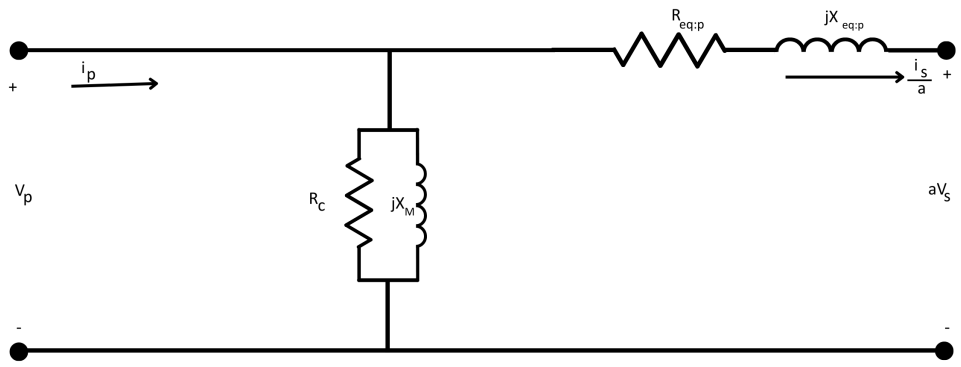

Figure 2.10: Approximated equivalent circuit, reference to primary winding

The excitation branch (R_c and X_M)has a very small current through it, around 2-3 % of the full load current of a typical transformer. Due to this, the simplified circuit works as well as the original model [31].

2.6 Magnetic properties

The core of the transformer is made from a ferromagnetic material. When an external magnetic field is applied to it, magnetic domains inside the material align themselves according to the field which makes the material magnetized. After removing the external magnetic field, the magnetic domains of the material do not realign themselves properly, some magnetization properties remain in the material. This property of the material is shown in the figure, where varying magnetic field strength is applied to a ferromagnetic material, and flux density B is plotted against the magnetizing force, from zero to peak (point A), and demagnetizing until saturation (point D), and finally bringing the flux density to zero (point F) which makes the hysteresis loop, which shows the energy loss during the magnetization and demagnetization of a material. This energy loss is called hysteresis loss [32].

The relation between flux density B and flux intensity H is defined as:

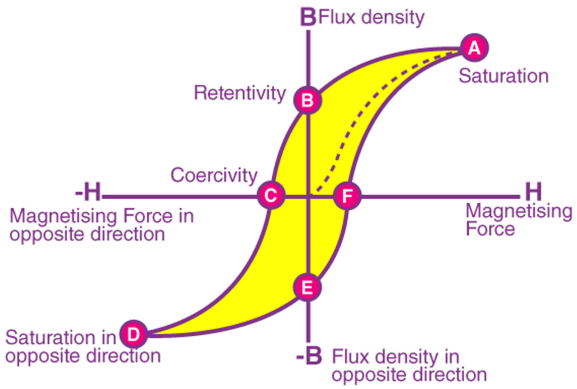

Figure 2.11: Hysteresis loop [32]

$$B = \mu_r \mu_0 H \tag{2.11}$$

where: μ_r = relative permeability of the material,
μ_0 = permeability in free space.

The relative permeability of free space in equation, 2.11 is $\mu_0 = 4\pi \cdot 10^{-7} \frac{H}{m}$. Magnetic material behaves linearly μ_r if is constant [5].

2.7 Power losses

The efficiency of power transformers varies from 97- 99 percent [33]. Transformers experience various type of losses that includes [31]:

1. Iron or core losses
2. Resistive or copper losses
3. Stray losses
4. Dielectric losses

2.7.1 Iron or core losses

In the transformers, magnetic lines of force are always changing their direction and value. The heat is produced because of the hysteresis loss in the magnetic material [18]. As these losses occur in the core of the transformer which is made of iron (ferromagnetic material), that is the reason to call them iron or core losses. In transformers when the voltage is applied on the primary side and the secondary side is an open circuit, it draws some of the current. This is called no-load current. The value of this no-load current is typically around 1 percent to 2 percent of the full load. The core losses are also called no-load losses because they are present when the transformer is connected to an open circuit as they are almost independent of the load [5]. Since these losses are due to the changing magnetic fields, they are produced in the transformer whenever primary windings are energized even when there is no secondary load on the windings [18]. Iron losses are further divided into [34]:

- Hysteresis losses
- Eddy current losses

Hysteresis losses

The losses that occur in the core due to the molecular friction caused by the changing polarity of the applied alternating current are called hysteresis losses. Whenever the magnetic field is reversed, the alignment of the molecular magnets is also reversed because some of the power is dissipated in the form of heat [35]. This behavior is explained in section 2.6, and also included in the numerical modeling. Hysteresis loss is the no-load loss that crops up in the transformer's core [5]. The total hysteresis loss P_h can be calculated by the given equation [33] [34]:

$$P_h = k_h B_{max}^{1.6} f V_{core} \tag{2.12}$$

where:

k_h = proportionality constant. Its value depends on the volume and quality of the core material that is being used in the transformer,
B_{max} = peak or maximum value of flux density B, and the value of the empirical exponent varies from 1.4 to 1.8 but its value is often given as 1.6 as for iron [33],
f = frequency of the current supplied,
V_{core} = volume of the core of the transformer.

Eddy current losses

Eddy current losses are one of the main losses in the transformer core. When the flux links with the closed circuit, Electromotive force (emf) is induced in the circuit. Since the core is made up of the conducting material so this emf induces a current in the metallic transformer core called eddy current. The value of this current depends upon two factors, the resistance of the circuit and emf around the circuit. This current is not useful for any work, and they produce a loss in the magnetic material, and due to this loss heat is produced in the core. These are called eddy current losses. The eddy current losses can be minimized by making the core with thin laminations or laminating the iron core. [33] [34]. The eddy current loss (P_e) can be calculated by the given relation [5]:

$$P_e = k_e B_{max}^2 f^2 \tag{2.13}$$

where:

k_e = coefficient of the eddy current, its value depends on the nature and characteristics of the magnetic material like the thickness of laminations, resistivity, and volume of the material of the core,
B_{max} = peak or maximum value of flux density B,
f = frequency of the current supplied.

Approximately half of the power losses that occur in the iron core are due to the eddy current losses and at no load, it can be as high as 61.5 % [5].

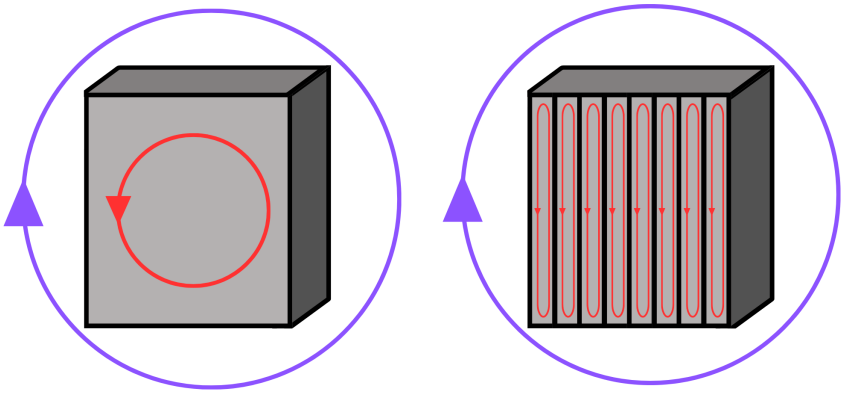

Figure 2.12: Effect of eddy current due to lamination on magnetic material

Figure 2.12 (left), shows the effect of induced eddy current by the red curve in a single material and after laminating the same material (right), while the applied coil current is

shown by the outside purple color. When magnetic material is laminated, the behavior of electrical conductivity changes from isotropic to anisotropic. Electrical conductivity becomes smaller in the direction of lamination due to the high resistance of the laminated material but electrical conductivity remains unchanged in other directions [5].

2.7.2 Resistive or copper losses

As the name indicates, these losses are due to the resistance of the primary and the secondary windings. Usually, transformer winding consists of hundreds of turns of fine copper wire that result in a high resistance value [35]. Resistive losses are also called copper losses because windings are normally made of copper. In this thesis, it will be called resistive losses to avoid confusion since the analytical model has copper windings while the numerical model uses aluminum windings.

Resistive losses are the main load losses and they vary with the load, so they are also called variable losses [34].

$$P_{Cu} = R_e I^2 \tag{2.14}$$

The magnitude of the resistive losses (P_{Cu}) depends upon the resistance of the windings (R_e) and the square of the current (I^2) flowing through the windings, which can be calculated using equation 2.14. Resistive losses can be minimized by reducing the resistance per unit length of the wires and this is done by using larger diameter conductors. In most transformers, resistive losses are twice as much as the core losses [35].

2.7.3 Stray losses

Leakage flux that links with the nearby conducting material such as the support structure of the transformer, will produce eddy currents that are converted into heat [33]. The losses that occur due to the presence of the leakage flux are called stray losses [34]. Stray losses include all of the other losses that cannot be included in any of the above categories [31]. The percentage of these losses as compared to the copper and iron losses is very small so they can be neglected [34]. In most of the machines, the stray losses are taken as 1 percent of the full load [31]. These losses are not included in the simulation model of this thesis.

2.7.4 Dielectric losses

The losses that occur in the transformer's insulating material which is in the solid insulations or in the oil of the transformer are called dielectric losses. When the quality of the insulation in the transformer decreases or gets damaged, the efficiency of the transformer is affected, and in the same way when the oil of the transformer deteriorates that also decreases the efficiency of the transformer [34]. Dielectric losses are not included in the simulation modeling of this thesis.

2.8 Skin effect and proximity effect

In DC current, the current distribution is uniform throughout the cross-section of the conductor but in AC current, due to changing magnetic field (H) results in inducing eddy current (I_{Eddy}). If the current increases, the magnitude of the magnetic field increases, which ends up in a more eddy current in the conductor. Eddy current is circulatory in nature as shown in figure 2.13. This eddy current has the opposite direction in the middle of the conductor while it has the same direction around the edges of the conductors, which cancels the current in the middle and reinforces a higher magnitude of current in the "skin" of the conductor [5]. Due to the skin effect, the intensity of the current is shown by the red color in figure 2.13.

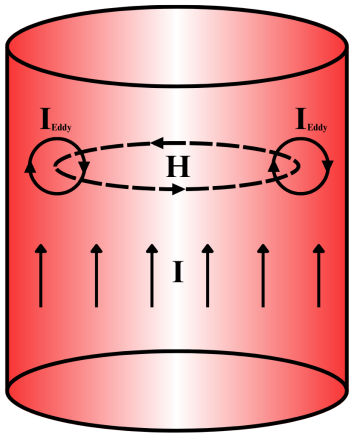

Figure 2.13: Effect of skin effect due to AC current in a conductor

The skin depth δ can be calculated using:

$$\delta = \sqrt{\frac{1}{\pi \mu_0 \mu_r \sigma_e f}} \tag{2.15}$$

where:
μ_0 = permeability in vacuum (constant),
μ_r = permeability in free space (constant),
σ_e = electrical conductivity of the conductor (material property constant),
f = frequency of the applied current.

When the AC current flows through the conductors that are placed in the vicinity of varying magnetic fields of each other, the current distribution of each individual conductor is affected due to induced eddy current in adjacent conductors. The apparent resistance of the conductors increases due to the eddy current [5]. When two current-carrying conductors are placed close to each other and current flow is in the same direction, the current distribution is higher at the farthest side of the conductors and vice versa as shown in figure 2.14 by red color.

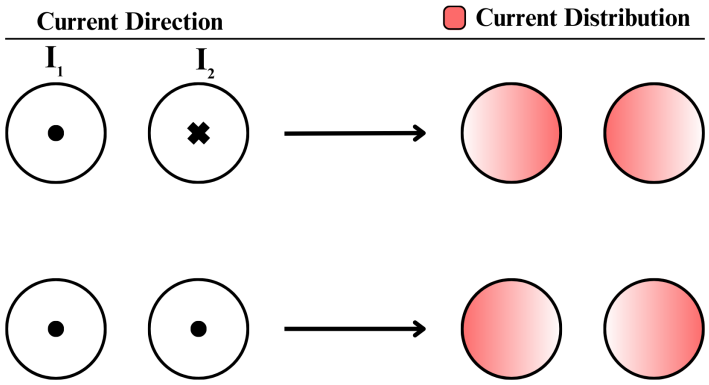

Figure 2.14: Proximity effect due to AC current

2.9 Heat Transfer

Heat is a form of energy, whenever there is a temperature difference between the medium, heat transfer occurs. The rate at which thermal energy flows from a higher body temperature to a lower body temperature is called the rate of heat transfer, heat flow, or heat exchange [17], [5]. In a transformer, heat transfer occurs through three modes:

- Conduction
- Convection
- Radiation

2.9.1 Conduction

The process through which the heat is transferred across a stationary medium (solid or fluid) due to temperature difference is called conduction. Almost in all types of transformers heat flows from the core and windings. From the core, heat can flow directly but in the case of the windings, heat flows through the insulation. In large transformers, heat flows through the small thickness of conductor insulation because at least one side of the insulation conductor must be connected to the cooling medium but in the case of small transformers, heat before reaching the cooling medium, may have to pass through the several layers of conductors and insulation materials [17]. It can be calculated using Fourier's law of heat conduction given in equation 2.16:

$$q = -k\Delta T \tag{2.16}$$

where:
q = local heat flux density in W/m^2,
k = material's conductivity in $W/(mK)$,
ΔT = temperature gradient in K/m.

2.9.2 Convection

Convection is the mode of transfer of heat from a solid material to a liquid or fluid [17] [5]. The fluid in the transformer is oil. The oil has an important mechanical property, which is the change in its volume with the change in temperature and pressure. This change of volume with the temperature provides required convective cooling [17].

In a transformer, the heat dissipation from the core and windings mainly occurs due to convection. When a hot surface that is to be cooled is immersed in the fluid, the heat from the hot body transfers to the cooling medium. This increases the temperature of the fluid and due to this, the density of the fluid decreases. This fluid (oil) in an oil-cooled transformer rises upwards and transfers its heat to outside ambient air with the help of a tank and radiators. The rising oil is then replaced by the cooler oil from the base and thus this circulation occurs continuously. The heat transfer from the transformer tank to the surrounding air occurs in the same way but the difference is that the warmed air does not come back after cooling, and the place of that air is occupied by the new fresh air. The convective heat transfer can be calculated by the following relationship [17]:

$$Q = hA(T_{surface} - T_{fluid}) \tag{2.17}$$

where:
Q = heat flow in W,
h = coefficient of heat transfer in $W/(m^2K)$,
A = surface area m^2,
$T_{surface}$ = surface temperature in K,
T_{fluid} = fluid temperature in K.

In equation 2.17, the calculation of heat flow (h) is very difficult as it depends on the geometry and the fluid properties, hence empirical approximations are used [17].

Free and forced convection

There are two types of convection: free or natural convection and forced convection. In free convection, fluid molecules move due to buoyancy force induced by differences in density and temperature gradient without external equipment for the movement of molecules [36].

Key differences between free and forced convection are given below in table 2.2:

Table 2.2: Free vs forced convection [36].

Free Convection	**Forced convection**
Movement of molecules solely due to density and temperature difference	Movement of molecules are due to external source
The rate of heat transfer is lower	The rate of heat transfer is much higher
Less complex, smaller size	Complex, and large in size
Flow can not be controlled, natural	Flow can be controlled with fan, pump, etc.

When an external source is used for (boosting) fluid flow, then it is considered forced convection.

Richardson number (Ri) is used for determining the dominant type of convection [5].

$$Ri = \frac{Gr}{Re^2} \tag{2.18}$$

In equation 2.18, (Gr) is the Grashof number which is a dimensionless number that approximated the ratio of buoyancy forces to viscous forces in a fluid given by:

$$Gr = \frac{g\beta\Delta T L^3}{\nu^2} \tag{2.19}$$

where:
g = gravitational constant,
β = thermal expansion,
ΔT = temperature difference between surface temperature and bulk temperature of the fluid,
L = vertical length,
ν = kinematic viscosity.

In equation 2.18, (Re) is Reynolds number that is a dimensionless number that helps in the prediction of the pattern of fluid flows and is given by:

$$Re = \frac{uL}{\nu} \tag{2.20}$$

where:
u = fluid velocity.

Substituting equations 2.19, 2.20 in equation 2.18 becomes:

$$Ri = \frac{g\beta\Delta TL}{u^2} \tag{2.21}$$

Using the Richardson number (Ri) the dominant type is estimated as:

$Ri << 1$ = forced convection,
$Ri >> 1$ = free convection,
$0.1 < Ri > 10$ = both.

2.9.3 Radiation

When the temperature of the body is higher as compared to its surroundings it radiates heat in the form of waves called radiation [17]. The heat dissipation from the tank of the transformer occurs through two modes of heat transfer, radiation, and convection. The radiators are also cooled down by radiation but it's less than that of convection because in radiators the fins are close to each other, so the entire surface of the radiators does not get involved in the heat transfer mechanism by radiation. Therefore, the effective area for radiation could be taken as the outside surface of the radiators. An object with temperature emits radiation, the power output is given by the Stefan–Boltzmann law as [5]:

$$P_{Radiation} = A\sigma T^4 \tag{2.22}$$

where:
A = area of the radiating surface,
σ = Stefan Boltzmann constant,
T = absolute temperature.

3 Literature Review

In this chapter, a brief history of the work done during the last few decades for analyzing trans-former thermal characteristics is explained precisely.

3.1 Thermal Losses

Thermal losses in transformers refer to the loss of energy during transformation in the form of heat. Core and Winding's losses are the two main categories of losses inside transformers. Core losses include hysteresis losses and eddy currents while Winding losses are usually due to the resistance of the windings. These losses reduce efficiency and life, therefore many models to estimate these losses were predicted in the past. In the literature review, some of the earliest works on the thermal stress of the transformer are discussed.

3.2 Earlier Work

The earliest work related to the hot spot temperature measurement was done by Stewart and Whitman in October 1944. They performed an extended series of thermal tests on different types of dry-type transformer coils and their hot-spot temperatures were calculated [5].

After that conventional winding temperature indicator devices were used to measure the temperature of the hottest region of the winding of a power transformer. These devices, rather than measuring the winding temperature directly, do the simulation of the hottest region of the windings directly. The accuracy of these devices is not reliable for all possible loading conditions because they can be calibrated only for one value of the load to measure the hot spot temperature. So, there was a need for a device that can measure the temperature of the transformer's winding directly for all the values of the load [37].

In 1984 W. J. McNutt, J. C. Mciver, and G. E. Leibinger used a commercial device fluoroptic fiber optic temperature sensors. Fluoroptic thermometers are used in various medical, scientific, and industrial laboratories to measure temperature. The sensor is based on a modeled disk having dimensions of 0.4mm (diameter) x 0.13mm (thickness). These sensors have never been used before in the transformer environment so immense

testing was required. Several thermal tests were conducted for a wide range of loading conditions and then temperature data were recorded from both methods, conventional measuring equipment and fluoroptic thermal sensors but experimental results show three types of potential data errors. After that corrective measures were taken and with the help of these fluoroptic thermometers accurate conductor temperature was obtained. Besides this, fiber optic sensors can also accurately measure temperature rise due to local loss densities [37].

In the early 1980s, fiber optical probes were introduced to measure the hot spot temperature of the windings of the transformer. Through this experimental technique real-time accurate values can be obtained but at the same time has two disadvantages as well. Since the exact location of a hot spot is not known so a minimum of eight sensors is required and secondly these sensors are very costly. After that several researchers developed mathematical models that can estimate the exact temperature and location of the hot spots. Heat transfer models were further added to find the local temperature rises. Two models were presented that simulate the total oil flow in the transformer. These combined models describe the global trans-former in a 2-dimensional(D) plane, and they can calculate the temperature of all kinds of windings (with any geometry) and wires and for all cooling methods [38].

Mohd Taufiq and Zhongdong have done three case studies to compare the hotspot temperature calculation methods using the IEEE loading guide. To measure the hot-spot temperature they have done a comparative study between the two methods that are Clause 7 and Annex G calculation method presented in the IEEE loading guide. With the help of various experimental evidence, they showed that the Annex G method is more complicated because it requires measured top oil and bottom oil temperature rise and that is not supplied by the manufacturer. While Clause 7 method is an inadequate hotspot temperature measurement method. So, for accurate hotspot temperature measurement of a transformer, improved specifications on thermal aspects are needed [39].

During the last ten years, many authors have used fiber optic probes to obtain possibly accurate transformer temperature values. In 2005 Dejan Susa, Matti Lehtonen, and Hasse Nordman proposed a general model that further explored the previous findings. They presented a new idea and focused on the nonlinear thermal resistance of the transformer oil. They introduced two transformer thermal models as top oil temperature model and the hot spot temperature model for more accurate temperature calculations. These thermal models were applied on three units of the transformers by varying load and then results were compared with the results of the experimental calculation and to the results obtained by the IEEE-Annex G method. It was concluded that the results of the thermal models work very well, especially for top oil temperature and the results obtained by the IEEE-Annex G method are accurate for hot spot temperature calculation only [2].

With the passage of time, various thermal models have been introduced to estimate the hot-spot temperature behavior and for this purpose, various temperature measurements

are obtained. These methods include thermocouple devices and fiber optic sensors. In 2007 a multi-point fiber optic sensor network was integrated into the transformer for the continuous monitoring of the hot spots in the windings, oil, and cellulose insulations. The authors demonstrated experiments for measuring the temperature with a fiber Bragg grating (FBG) network. This sensing system can show the real-time status and aging behavior of the transformer [40].

In 2010, Lee, Abdullah, Jofriet, and Dhiru Patel did the thermal modeling for foil winding and the behavior of temperature is determined by the finite element method (FEM) and physical testing. With the help of the modeling, non-uniform power losses were also calculated. The two-dimensional(2D) thermal model involves conduction, convection, and radiation. They also did the modeling in COMSOL. This study was very helpful for manufacturers [41].

In 2012, Ding and Ning did the modeling of a 3D dry-type transformer in SOLIDWORKS and calculated the temperature rises in windings and the iron core with the theory that was based on conduction. The model was then imported in COMSOL for simulation of temperature field analysis and then the hot spot was obtained. The experiments showed that low voltage winding of dry-type transformer has a hot spot and the study also represents that online monitoring and optimization can increase the life of the transformer [42].

In 2014, Arjona, Hernandez, Escarela-Perez, and Melgoza presented a thermal model that is solved with the finite element method (FEM). The FEM method is used to solve the axisymmetric model of the three-phase transformer. The focus of this model is on the analysis of thermal behavior (conduction, convection, and radiation) and fluid dynamics. The paper compares the simulation results of the temperature rise when the transformer is operating at no load and full load. The first Simulation was done for the full load case while considering the core and winding losses as the heat source while the second simulation is for the no-load case while considering only the core losses as the heat source. In the case of loading simulation results shows higher temperatures than the no-load case and the loaded model gives useful and detailed data that can be used by the users and manufacturers to look over the thermal loading of the transformer before making the prototype [43].

4 Methodology for hot-spot analysis

This section will describe thermal-electrical analogy for analytical modeling. Non-linearity in thermal behavior is characterized by defining nonlinear thermal resistance. A simple thermal model of top oil temperature is defined and later verified. The data used for modeling thermal behavior is provided by "Skagerak Kraft" of the transformer from one of their power plant. Skagerak provided the 3 months of active and reactive power data along with top oil and water temperatures for the 118 MVA transformer from the power plant in CSV (Comma Separated Values) format. This is a typical format used to store data because it is plain text files and easy transportation between different programs.

4.1 Transformer Parameters

The transformer used for the Analytical model is:

Table 4.1: Parameters of Transformer used for Analytical modeling

Parameter name	**Value**
Rated Power	118 (MVA)
Frequency	50 (Hz)
Phase	3
Primary voltage	15 (kV)
Secondary voltage	308 (kV)
Primary current	4550 (A)
Secondary current	222 (A)
Mass of oil	25000 (kg)
Mass of core, winding and lid	90000 (kg)
Mass of box and coolers	13000 (kg)
Cooling method	OFWF
Short circuit losses	365 (kW)

4.2 Thermal Analytical Model

In this section, the thermal data from the real transformer is used for the estimation of the thermal time constant using the machine learning package in *Julia* and used in the modified IEEE method for predicting the thermal behavior of the transformer.

4.2.1 Electrical-Thermal analogy

The basic thermal-electrical analogy is presented below [44]:

$$q \times dt = C_{th} \times dT + \frac{T - T_{amb}}{R_{th}} \times dt \tag{4.1}$$

where:

q = heat generation,
C_{th} = thermal capacitance,
T = temperature,
T_{amb} = ambient temperature,
R_{th} = thermal resistance.

The basic thermal equation 4.1 can be rewritten as:

$$q = C_{th} \times \frac{dT}{dt} + \frac{T - T_{amb}}{R_{th}} \tag{4.2}$$

A fundamental RC (Resistor Capacitor) circuit, where Resistance and capacitor are connected in parallel, is shown in figure 4.1.

In figure 4.1:

i = current,
C = capacitance (electrical),
T = temperature,
u = voltage,
R = resistance (electrical).

Using Kirchhoff's law for the circuit in figure 4.1:

$$i = C + R \tag{4.3}$$

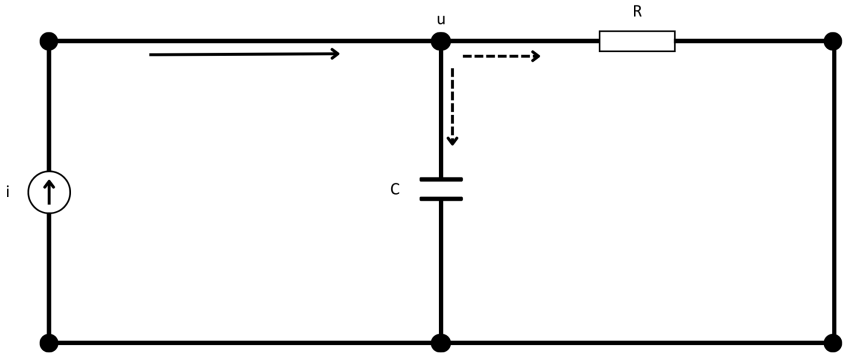

Figure 4.1: Fundamental RC circuit

Using Ohm's law, equation 4.3 becomes:

$$i = C \times \frac{du}{dt} + \frac{u}{R} \tag{4.4}$$

By comparing the basic thermal equation 4.2 and electrical equation 4.4, a thermal-electrical analogy can be obtained, presented in table 4.2.

Table 4.2: Thermal-electrical analogy [44].

Thermal	**Electrical**
Heat generated (q)	Current (i)
Temperature (T)	Voltage (u)
Thermal resistance (R_{th})	Resistance (R)
Thermal capacitance (C_{th})	Capacitance (C)

Thermal resistance (R_{th}) shows the ability to resist the heat flow while thermal capacitance (C_{th}) is the property of a material to store heat. Thermal-electrical analogy circuit is shown in figure 4.2

4.2.2 Top oil thermal model

The basic circuit for the top oil thermal model is presented in figure 4.3, based on thermal-electrical analogy presented in sec 4.2.1. Where q_{tot} is an ideal heat source, represents the total losses in the form of heat, which is the sum of load losses and no-load losses.

The rest of the quantities in figure 4.3 are as follows:

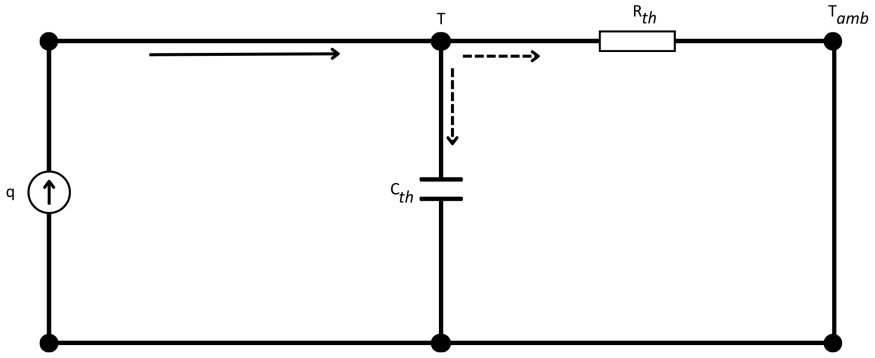

Figure 4.2: Thermal-electrical analogy circuit

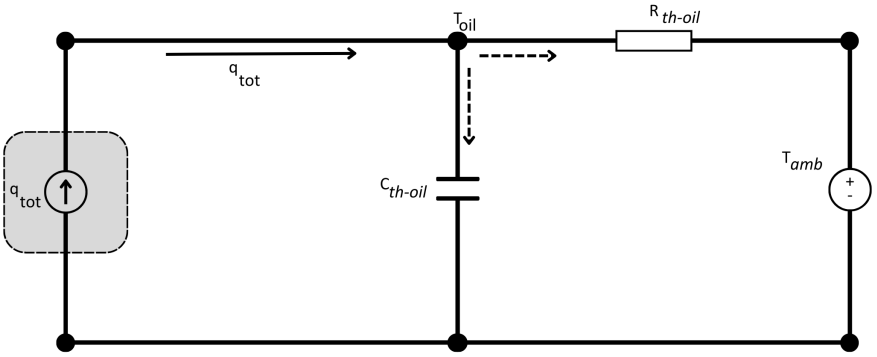

Figure 4.3: Top oil thermal model circuit

C_{th-oil} = thermal capacitance of oil,
T_{oil} = oil temperature,
T_{amb} = ambient temperature, represented by an ideal heat source,
R_{th-oil} = thermal resistance of the oil.

The thermal differential equation for the figure 4.3 is:

$$q_{tot} = C_{th-oil} \times \frac{dT_{oil}}{dt} + \frac{T_{oil} - T_{amb}}{R_{th-oil}} \tag{4.5}$$

rearranging equation 4.5:

$$C_{th-oil} \times \frac{dT_{oil}}{dt} = q_{tot} - \frac{T_{oil} - T_{amb}}{R_{th-oil}} \tag{4.6}$$

or

$$(C_{th-oil} \cdot R_{th-oil}) \times \frac{dT_{oil}}{dt} = q_{tot} \times R_{th-oil} - (T_{oil} - T_{amb}) \tag{4.7}$$

Time constant

The time constant of an electrical RC circuit, in figure 4.1, is the time required to charge a capacitor to 63.2 % of the full charging. It is defined as the product of electrical resistance and electrical capacitance. Mathematically written as:

$$\tau = R \cdot C \tag{4.8}$$

The thermal time constant is defined similar to the electrical time constant using a thermal-electrical analogy. Generally, 63 % change in temperature occurs in one time constant regardless of initial and final temperatures [44].

$$\tau_{th} = R_{th} \cdot C_{th} \tag{4.9}$$

where:

τ_{th} = thermal time constant in minutes,
R_{th} = thermal resistance in K/W,
C_{th} = thermal capacitance $W{\cdot}s/K$,

Hence, equation 4.7 becomes:

$$\tau_{th-oil} \times \frac{dT_{oil}}{dt} = q_{tot} \times R_{th-oil} - (T_{oil} - T_{amb}) \tag{4.10}$$

The final simple differential equation for top oil after rearranging 4.10 becomes:

$$\frac{dT_{oil}}{dt} = \frac{1}{\tau_{th-oil}} \cdot (q_{tot} \times R_{th-oil} - (T_{oil} - T_{amb})) \tag{4.11}$$

4.2.3 Assumptions in top oil thermal model

The data available for modeling has only active, reactive powers and temperature of oil and water in the form of comma-separated values (CSV) measurements. Other relevant data in hand were basic Ratings and masses of the oil and transformer. So, there were assumptions made to use the basic top oil thermal model presented.

- The top oil temperature was available but not ambient temperature, however using cooling water the temperature difference was calculated for modeling. The temperature of cooling water T_{water} replaces the ambient temperature T_{amb} in Equation 4.11.
- Total losses q_{tot} is an important parameter and thermal behavior depends on how the losses vary with temperature, with very less information it was not possible to calculate exact total losses but since we have active power and reactive power, we can use them instead of losses to estimate the oil time constant.
- Two different approaches were used to verify the model top oil temperature.
- Active power losses of Transformer in pu, P_{t-loss} is calculated using transformer nameplate as:

$$E_r = 0.31\% \tag{4.12}$$

  E_r shows the percentage of short circuit losses of the transformer at full load.

$$P_k = 0.31\% \times 118MVA = 365kW \tag{4.13}$$

  P_k shows the active power losses of the transformer in the form of heating at full load. P_{k-pu} in the equation shows the losses of the transformer at full load e.g., 1 p.u.

$$P_{k-pu} = 0.0031pu \tag{4.14}$$

  1. Using active power losses of transformer in pu, $P_{t-loss-pu}$ replaces the total losses q_{tot} in equation 4.11.
  2. Using Reactive power of transformer in pu, Q_{t-pu} replaces the total losses q_{tot} in equation 4.11.

- Modified IEEE method is used for prediction of the hotspot temperature, and it is simulated in *Matlab* where all the equations from 4.15 - 4.18 are solved numerically using Runge-Kutta method. Three different cases are shown in the simulation results:

1. Under load when the loading factor $K = 0.85$.
2. Rated load when the loading factor $K = 1$.
3. Over-load when the loading factor $K = 1.2$.

4.2.4 Transformer data processing for thermal model

The data provided by Skagerak Kraft was based on CSV files containing active power (MW), reactive power ($MVAr$), oil temperature ($^{\circ}C$) and cooling temperature ($^{\circ}C$). The data was based on around three months of samples but with varying sampling rates for each file. That means they must be synced before processing. CSV files are not practical for visualizing and working, hence at first instance, the data was converted from CSV files to Excel columns data set using the Microsoft Excel function name "split columns by Delimiter" and saved as text to columns. Brief summary of the data processing steps are :

- The data was having discontinuities at some time frames in one or more data sets. Data from one week of December 2022 was chosen for processing because of fewer discontinuities and contains the behavior from initial to steady state temperature.
- The cells with "NaN" (Not a Number) must be replaced with actual values.
- Repetitive values were removed using Excel.
- Data was further narrowed down to 24 hours time frame, and the chosen day has the highest fluctuations in temperature.
- Active and Reactive powers were converted into per unit (pu) values in Excel using base 118 (MVA).
- The data was interpolated in MATLAB to sync all in the same 24-hour time frame, 86400 discrete points in seconds for one data set e.g., per unit active power of the Transformer (P_{t-pu}, $86400 \times 6 = 518400$) in total.
- Interpolated data was processed in Julia using neural network differential equations to make a model fit for the data with the help of 8000 iterations to get a good fit.
- With the help of neural network differential equations, the thermal time constant (τ_{th-oil}) of the oil is estimated along with the nonlinear thermal resistance of the oil (R_{th-oil}).
- The thermal time constant (τ_{th-oil}) is used in the modified IEEE method equation 4.17, 4.18 for estimation of hotspot temperature. Modified IEEE methods are only used for hotspot estimation, however, the complete model including top-oil is given below in equation 4.15, 4.16.

4.2.5 Neural ODE details

The "flux" is a very powerful tool, from the machine learning library of *Julia* and it provides the tools that are used for building and training the neural network. It comes with many built-in tools such as "Flux.params" and "Flux.train" are the functions used in this thesis for training data for curve fitting.

The thermal time constant (τ_{th-oil}) of the oil is estimated and the nonlinear thermal resistance of the oil (R_{th-oil}) are the two parameters required for estimation based on the thermal equation 4.11, which is defined in *Julia*, complete code can be accessed through appendix C.

The function "Flux.params" used for extracting the trainable parameters of the model:

```
Flux.params(p)
```

In this example, the "flux.params" is used for extracting the trainable parameters from model "p", which must be defined earlier.

The function "Flux.train" used for training machine learning model which is defined as [45]:

```
Flux.train!(loss_function, model, data, optimizer, cb)
```

where:
The "loss function" is defined before because "train function" measures the error and it needs this function to measure the amount of error. The "model" is the neural network model which has to be trained. The "data" is the training data that is based on the number of "epochs" provided. After each iteration, the error is assigned a weight to minimize it. the weightage assigned is defined by the "optimizer". In this thesis the optimization algorithm used is "adamax", which updates the parameters of the machine learning by assigning them weightage during "flux.train" call. The "cb" is an additional input which is called "call back" function, used for monitoring the progress [45].

One "epoch" means one full iteration through the entire dataset, for this code in appendix C, 8000 "epochs" were used to attain an acceptable limit of losses, losses at the end of 8000 "epochs" reduced to 127.37.

4.2.6 Modified IEEE method for Hotspot

An increase in loading will result in an increase in top oil temperature. The modified IEEE method includes the ambient temperature variations into the original IEEE top oil method. Ultimate top oil temperature rise over ambient temperature is given by [46]:

$$\Delta T_{oil,u} = \tau_0 \frac{dT_{oil}}{dt} - T_{amb} + T_{oil} \tag{4.15}$$

where:
$\Delta T_{oil,u}$ = ultimate top oil temperature rise over ambient in degree Celsius,
τ_0 = top oil time constant in hours,
T_{oil} = dynamic top oil temperature in degrees Celsius,
T_{amb} = ambient temperature in degrees Celsius.

also,

$$\Delta T_{oil,u} = \Delta T_{oil,R} (\frac{K^2 R + 1}{R + 1})^n \tag{4.16}$$

where:
$\Delta T_{oil,R}$ = rated top oil temperature rise over ambient in degree Celsius,
K = load current per unit,
R = ratio of load to no load losses,
n = exponential that defines nonlinearity.

The top oil temperature then becomes the input for the estimation of hotspot temperature [46]:

$$\Delta T_{hst,u} = \tau_{wnd,R} \frac{dT_{hst}}{dt} + T_{hst} - T_{oil} \tag{4.17}$$

$$\Delta T_{hst,u} = \Delta T_{hst,R} (K)^{2m} \tag{4.18}$$

where
$\Delta T_{hst,u}$ = ultimate hotspot oil temperature rise over top oil in degree Celsius,
$\Delta T_{hst,R}$ = rated hotspot oil temperature rise over top oil in degree Celsius,
T_{hst} = dynamic hotspot temperature in degree Celsius,
$\tau_{wnd,R}$ = winding time constant in minutes,
m = exponential for non linearity.

The results are attached in simulations.

4.3 Introduction to COMSOL

COMSOL Multiphysics® is a software based on Finite Element Method (FEM) that can combine multiple physics for many different engineering problems by solving differential equations. COMSOL is used in this thesis to build a 2D FEM transformer model because of two main reasons.

1. Possibility to couple Electromagnetism and thermodynamics.
2. University has a license to this software.

This section is dedicated to simulation models in COMSOL Multiphysics®, defining geometry, material properties, domain conditions, and various boundary conditions. Two different models are used in this master thesis, The first model that is used in this thesis is a three-phase E-core transformer which has multiple single-turn coils to generate the effect of electromagnetics. The main purpose of this model is to analyze skin and proximity effects in transformer windings. The second model presented in this thesis is also a three-phase E-core transformer but with multi-turn coil approximation. Multi-turn coil approximation has uniform current density and neglects the proximity effect and skin effects. This is used to model thermodynamics.

4.3.1 Boundary conditions

COMSOL Multiphysics® has numerous physical systems that are generally defined with the following general differential equation [47]:

$$e_a \frac{\partial^2 u}{\partial t^2} + d_a \frac{\partial u}{\partial t} + \nabla \cdot (-c_d \nabla u - \alpha u + \gamma) + \beta \cdot \nabla u = F_s \tag{4.19}$$

here e_a represents mass coefficient, d_a is used for damping coefficient/ mass coefficient, c_d is the diffusion coefficient, α is the absorption coefficient while β is convection coefficient. γ is representing (conservative flux) source and F_s also represents general source term [47]. u is a (general) dependable parameter. Equation (4.19) represents a general partial differential equation which can have different meanings and different units according to the physics.

For instance, In the heat transfer domain, F_s represents a heat source in (4.19) and u is representing temperature. ∇ is a mathematical vector operator gradient. Gradient of a scalar function $F(x,y,z)$ is given by [48]:

$$\nabla F(x,y,z) = \left[\frac{\partial F_1}{\partial x}, \frac{\partial F_2}{\partial y}, \frac{\partial F_3}{\partial z} \right] \tag{4.20}$$

The gradient of a scalar-valued function $F(x,y,z)$ in (4.20) is a vector that points to the function F_1 in x direction, F_2 in y direction and F_3 in z direction respectively. The symbol $\nabla\cdot$ (nabla dot) in (4.19) is called divergence and the divergence of a vector function $F(x,y,z)$ is given by [48]:

$$\nabla \cdot F(x,y,z) = \left[\frac{\partial F_1}{\partial x} + \frac{\partial F_2}{\partial y} + \frac{\partial F_3}{\partial z}\right] \tag{4.21}$$

The divergence '$\nabla\cdot$' in (4.21) of a vector $F(x,y,z)$ is a scalar quantity that represents the aggregate of "outward flow" of the field in a particular direction. Another term that is used parallel with divergence is a mathematical operator 'curl' which is not in the (4.21). The mathematical operator 'curl' is denoted by '$\nabla\times$' (nabla cross) is a vector operator and 'curl' of a vector function $F(x,y,z)$ is given by [48]:

$$\nabla \times F(x,y,z) = \left[\frac{\partial F_3}{\partial y} - \frac{\partial F_2}{\partial z}, \frac{\partial F_1}{\partial z} - \frac{\partial F_3}{\partial x}, \frac{\partial F_2}{\partial x} - \frac{\partial F_1}{\partial y}\right] \tag{4.22}$$

The 'curl' of a vector function $F(x,y,z)$ is a vector quantity that shows the rotation around a specific point. The vector function on the left side of the equation (4.21) & (4.22) is defined as [48]:

$$F(x,y,z) = [F_1(x,y,z), F_2(x,y,z), F_3(x,y,z)] \tag{4.23}$$

In COMSOL there are three types of shape functions available for the numerical modeling of magnetic field domains and heat flow:

- Linear
- Quadratic
- Cubic

This is used in the discretization of the governing equations to solve physics problems. By default quadratic function is selected for the magnetic field while the heat flow domain uses linear discretization. In this thesis, default settings of discretization are used in all models.

4.3.2 Magnetic fields

Some of the equations that are used for numerical modeling in this thesis from magnetic field interface in COMSOL Multiphysics® are presented in this section. In static cases, Amperes law can be stated as [47]:

$$\Delta \times \mathbf{H} = \mathbf{J} \tag{4.24}$$

where:
$\mathbf{H}$ = magnetic filed intensity in A/m,
$\mathbf{J}$ = current density in A/m^2.

By using the definition of fields, the magnetic flux density ($\mathbf{B}$) is given by [47]:

$$\mathbf{B} = \Delta \times \mathbf{A} \tag{4.25}$$

where:
$\mathbf{B}$ = magnetic flux density in T,
$\mathbf{A}$ = magnetic vector potential in Vs/m.

Current density for the static case ($\mathbf{J}$) [47]:

$$\mathbf{J} = \sigma_e \mathbf{v} \times \mathbf{B} - \sigma_e \Delta V + \mathbf{J}_e \tag{4.26}$$

where:
$\mathbf{v}$ = velocity of the conductor in m/s,
V = electric scalar potential in V,
σ_e = electrical conductivity in S/m,
$\mathbf{J}_e$ = externally generated current density, e.g., in coils, represented in A/m^2.

Current density ($\mathbf{J}$) for the frequency domain analysis, assuming time-harmonic fields [47]:

$$\mathbf{J} = \sigma_e(\mathbf{E} + \mathbf{v} \times \mathbf{B}) + (j\omega\mathbf{D} + \mathbf{J}_e) \tag{4.27}$$

where:
$\mathbf{E}$ = electric field in V/m,
$\mathbf{D}$ = electric displacement in C/m^2,
ω = angular frequency in rad/s.

Transformer is surrounded by air, which can be modeled using Ampere's law domain with some simplifications. A big rectangular geometry is used to model the air around the transformer. The size of the geometry of the air domain is several times larger than the transformer because a smaller size may have problems with the magnetic flux being reflected back with the boundaries. By default, all outer edges have the boundary condition "Magnetic Insulation" given below [5]:

$$n \times \mathbf{A} = 0 \tag{4.28}$$

where:
$\mathbf{A}$ = magnetic potential in (Wb/m).

The air and the core domains are modeled using Ampere's law but a simplified version of equation 4.27 is used for current density ($\mathbf{J}$) by assuming $\mathbf{v} = 0$ and ignoring the external source of current density ($\mathbf{J}_e = 0$), as given below in equation 4.29:

$$\mathbf{J} = \sigma_e \mathbf{E} + j\omega \mathbf{D} \tag{4.29}$$

Coils are modeled by using the coil domain available in the Magnetic field interface. External current density of coils ($\mathbf{J}_e$) is included in the equation 4.27 and for homogenized multi-turn approximation ($\mathbf{J}_e$) is defined as [47]:

$$\mathbf{J}_e = \frac{NI_{cir}}{A_{coil}} \cdot e_{coil} \tag{4.30}$$

where:
N = number of turns in windings (only when homogenized multi-turn approximation is used),
I_{cir} = current from the external circuit connected to the coils,
A_{coil} = cross-sectional area of each winding,
e_{coil} = voltage across the windings.

4.4 Electric circuits

The windings of the transformer were modeled using coils domains in a "Magnetic Field" interface but their connections with each other and coil excitation were provided through an external voltage source using an "Electrical Circuit" interface because it provides more control for three-phase connections as well as offer's multiple power sources. When this physics is added, it automatically adds a default ground node with node number zero (0),

this default node was used in this thesis. Only three electrical components were used in this physics as below:

- Voltage Source
- Resistor
- External I Vs. U

and the connections of these components can be seen in figure 4.4 for a three-phase transformer. Each phase consists of the primary circuit consisting of a voltage source (V), small connection resistance (R_e), and external coupling component "I vs U" for connecting primary windings. This resistance (R_e) is added because Comsol does not allow the connection of a source directly to an external "I vs U" component. The secondary circuit consists of an external coupling "I vs U" with secondary coils and load resistance (R_{Load}).

The Voltage source offers multiple types of sources but "sine source" and "AC -source" were used in this thesis for the time domain and Frequency domain analysis. Both "sine source" and "AC -source", work similarly but in AC source, frequency is defined as a global parameter that must be entered through the solver configuration [47].

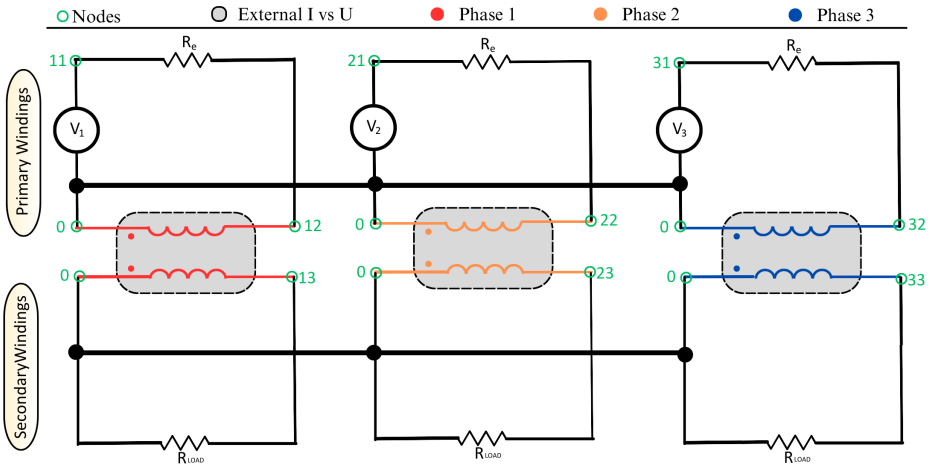

Figure 4.4: Three phase transformer circuit

The external "I vs U" component is used for external coupling (coupling with a component that is outside the "electrical circuit" physics). It connects an arbitrary voltage measurement as a voltage source between two nodes. The resulting current is measured between the two nodes of the connected circuit and coupled back as a current source in the context of voltage measurement [47]. In each phase, there are two of these components are connected and coupled with respective primary and secondary windings as shown in figure 4.4.

Table 4.3: Input Parameters for "Electrical Circuit" Physics COMSOL

Parameter	Value	Connection nodes	Unit
V_1	$6600\sqrt{\frac{2}{3}}@-120deg$	0-11	V
V_2	$6600\sqrt{\frac{2}{3}}@0deg$	0-21	V
V_3	$6600\sqrt{\frac{2}{3}}@120deg$	0-31	V
gnd	0	0-11, 0-12, 0-13 0-21, 0-22, 0-23 0-31, 0-32, 0-33	–
R_e	1	11-12, 21-22, 31-32	$m\Omega$
R_{Load}	105.8	0-13, 0-23, 0-33	Ω

The frequency of the system is globally defined as $50Hz$. The connection of the windings is start on both the primary and secondary side, including external "I vs U" coupling can be seen in figure 4.4 and values of the components are given in table 4.3. $R_{Load} = V_L^2/S$, The output line voltage $V_L = 23kV$ and rated apparent power $S = 5MVA$ results $R_{Load} = (23kV)^2/5MVA = 105.8\Omega$ [5].

4.4.1 Heat Transfer

Heat is a form of energy that transfers from one medium to another due to temperature difference [49].

The general heat transfer equation in Comsol is defined as [47]:

$$\rho C_p \frac{\partial T}{\partial t} + \rho C_p \mathbf{u} \cdot \nabla T - \nabla \cdot \mathbf{q} = Q \tag{4.31}$$

For the steady-state analysis, the temperature does not change with time ($\frac{\partial T}{\partial t} = 0$) and the general equation 4.31, after excluding the time derivative becomes:

$$\rho C_p \mathbf{u} \cdot \nabla T - \nabla \cdot \mathbf{q} = Q \tag{4.32}$$

where:
ρ = density in kg/m^3,
C_p = heat capacity in $J/kg \cdot K$,
$\mathbf{u}$ = velocity field, either defined analytically or automatically computed in the fluid domain, in m/s,
T = temperature in K,
$\mathbf{q}$ = conductive heat flux, in W/m^2,

Q = heat source or heat sink, more than one heat source can be defined in separate physics, in W/m^3.

In equation 4.32, conductive heat flux ($\mathbf{q}$) is defined as

$$\mathbf{q} = -k\nabla T \tag{4.33}$$

where:
k = thermal conductivity in W/mK

Comsol has a heat transfer interface for both solids and fluids which can be included in separate physics or fluid can be added as a domain in existing heat transfer in solid physics. Both approaches work the same but the latter method is used in this thesis as it is less messy and saves computational costs. The heat source in both solids and fluids is based on the same equation 4.32 but the heat source (Q), is defined differently. In solids [5]:

$$Q = Q_0 + Q_{ted} \tag{4.34}$$

where:
Q_0 = distributed heat source, which can be defined analytically or coupled with other physics that causes heat and is solved simultaneously in W/m^3,
Q_{ted} = thermoelastic damping, in W/m^3.

Thermoelastic damping is ignored in this thesis during numerical modeling because its effect is negligible at $50Hz$ and may add unnecessary computational costs.

In fluids [5]:

$$Q = Q_0 + Q_p + Q_{vd} \tag{4.35}$$

where:
Q_p = pressure work in W/m^3,
Q_{vd} = viscous dissipation in W/m^3,

In equation 4.35, pressure work (Q_p) is ignored because it considers the heat generation due to the adiabatic compression while viscous dissipation (Q_{vd}) accounts for the heat due to viscous stress in fluids which is also neglected in this thesis.

By default, outer edges have the boundary condition *Thermal Insulation* which is defined by the equation 4.36 :

$$-\mathbf{n}\cdot\mathbf{q} = q_0 \tag{4.36}$$

where:
$\mathbf{n}$ = normal vector at the boundary,
q_0 = inward heat flux, normal to the boundary, in W/m^2.

The inward heat flux (Q_0) is the sum of contributions from different heat transfer processes (e.g., radiation and convection). By default, inward heat flux (Q_0) in equation 4.36 is zero which behaves as *thermal insulation* [47]. This default condition behaves as the walls on the sides of the big rectangular geometry of the air but two of the sides (top and bottom) are replaced with boundary condition *Inflow* and *Outflow*. If outer edges are perfected sealed and *thermal insulation*, then the temperature will keep rising during simulation [5]. *Inflow* boundary condition is used for the exterior fluid domain and defined as [47]:

$$-\mathbf{n}\cdot\mathbf{q} = \rho\Delta H\mathbf{u}\cdot\mathbf{n} \tag{4.37}$$

where:
H = enthalpy in J/Kg.

Since in this thesis, all modeling performed in two-dimensional geometry and the thickness of the domain in out-of-plane direction (d_z) is not included in the equation 4.37, however for the three-dimensional modeling, it must be multiplied on the right-hand side of the equation 4.37. The enthalpy variation (ΔH) depends on the temperature difference between ($T\&T_{ustr}$) and the pressure difference between ($p\&p_{ustr}$), defined as [47]:

$$\Delta H = \Delta H_T + \Delta H_p \tag{4.38}$$

Change in enthalpy due to temperature is given by:

$$\Delta H_T = \int_{T_{ustr}}^{T} C_p dT \tag{4.39}$$

While the change in enthalpy due to pressure is given by:

$$\Delta H_p = \int_{p_{ustr}}^{p} \frac{1}{\rho}(1-\alpha_p T)dp \tag{4.40}$$

Substituting equations 4.39, 4.40 in equation 4.38 becomes:

$$\Delta H = \int_{T_{ustr}}^{T} C_p dT + \int_{p_{ustr}}^{p} \frac{1}{\rho}(1 - \alpha_p T) dp \tag{4.41}$$

where:
T = temperature in K,
T_{ustr} = upstream temperature, this is replaced with ambient temperature ($293.15K$) for modeling in this thesis, in K,
p = contact pressure in Pa,
p_{ustr} = upstream absolute pressure, this is replaced with ambient pressure ($1atm = 131325Pa$), for modeling in this thesis, in Pa,
α_p = coefficient of thermal expansion in $1/K$.

The coefficient of thermal expansion in (α_p) equation 4.41 is defined as[47]:

$$\alpha_p = -\frac{1}{\rho}(\frac{\partial p}{\partial T}) \tag{4.42}$$

For ideal gases, the above equation 4.42, can be simplified as:

$$\alpha_p = \frac{1}{T} \tag{4.43}$$

Inflow boundary condition is applied to the bottom of the air geometry, while *Outflow* boundary condition is applied to the opposite side (top) of the air geometry, which can be defined as:

$$-\mathbf{n} \cdot \mathbf{q} = \mathbf{0} \tag{4.44}$$

Using heat transfer, boundary condition *Diffuse surface* is applied to all the surfaces of the transformer model. It reflects radiative intensity in all directions. It adds radiative heat source contribution q as:

$$q = \varepsilon(G - e_b(T)) \tag{4.45}$$

where:
ε = surface emissivity,
G = surface irradiation, in W/m^2,
$e_b(T)$ = black-body hemispherical total emissive power, in W/m^2.

By default, the ambient temperature was defined as $293.15K$, which was replaced with variable (T), because the temperature is a dependent variable in the Comsol heat transfer

interface. By doing so, Comsol finds ambient temperature from the surfaces of the transformer. By default, emissivity (ε) was set to take from material properties, and replaced with a fixed value of 0.8 for all surfaces.

4.5 Laminar Flow

Laminar flow is used to model the flow of single-phase fluids. It is used where the velocity of the fluid is smooth and ordered. This physics is applied to the air domain since it is modeled as fluid in this thesis. Laminar flow is based on the Navier Strokes equation given below [5]:

$$\rho(\mathbf{u}\cdot\nabla)\mathbf{u} = \nabla\cdot(-p\mathbf{I}+\mu(\nabla\mathbf{u}+(\nabla\mathbf{u})^T)-\frac{2}{3}\mu(\nabla\cdot\mathbf{u})\mathbf{I})+\mathbf{F}+\rho\mathbf{g} \tag{4.46}$$

where:
I = identity matrix,
F = external forced acting on the fluid, in N/m^3,
g = gravitational acceleration, in m/s^2.

Laminar flow is only solved in steady state study, that's why time derivative is not included in equation 4.46. For specific equation 4.46, T does not stand for temperature but it is used for *transpose*. Outer edges of the transformer and air boundary, by default, are considered as *Walls*, which means that the velocity cannot enter or exit from there and velocity is zero. In Comsol *Wall* equation can be written as [47]:

$$\mathbf{u} = 0 \tag{4.47}$$

However, boundary conditions on the bottom of the rectangular geometry of air were replaced with *Inlet* and for the exit of the fluid from the top, *Wall* is replaced with *Outlet* boundary. *Inlet* boundary condition is defined is Comsol as [47]:

$$\mathbf{u} = -U_0\mathbf{n} \tag{4.48}$$

where:
$\mathbf{n}$ = normal vector ,
U_0 = normal inflow velocity, default = 0 , in m/s

Outlet boundary condition is defined is Comsol as [5]:

$$(-p\mathbf{I}+\mu(\nabla\mathbf{u}+(\nabla\mathbf{u})^T)-\frac{2}{3}\mu(\nabla\cdot\mathbf{u})\mathbf{I})\mathbf{n}=-(p_0+p_{hydro})\mathbf{n} \tag{4.49}$$

where:
p_0 = absolute pressure, in this thesis ($p_0 = 0$) , in Pa
p_{hydro} = fluid pressure due to gravity , in Pa.

The left side of the equation 4.49, is based on equilibrium forces like Naiver Stokes equation 4.46 while the right side of equation 4.49, is based on forces due to pressures. Fluid pressure (p_{hydro}) compensates the gravity pressure at the reference point ($0Pa$), provided that density is constant.

$$p_{hydro}=\rho_{ref}g\cdot(\mathbf{r}-\mathbf{r}_{ref}) \tag{4.50}$$

where:
$\mathbf{r}$ = position in the geometry,
$\mathbf{r}_{ref}$ = reference position (0,0).

4.6 Geometry

This section explains the steps for building the transformer model in COMSOL Multiphysics®. The geometry of the 2D three-phase transformer is shown in figure 4.5, the air domain was built multiple times larger than the transformer to exclude air behavior as infinity large free space (a), while (b) shows the zoomed-in view of transformer only with the labeling of primary and secondary windings.

Complete details for the geometry parameters are given in table 4.4, Core was built in two parts, equal identical geometries, and later unioned together as one. The single winding turn was built first and the rest of the turns were added using union operation. Since all the turns were built in geometry instead of approximation, the resulting model becomes very detailed and consists of 1205 domains in total. 1200 domains out of 1205 were used for only windings, this was necessary for accurate results but it's very computationally expensive. Zoomed-in view of the windings shows the details inside the windings in figure 4.6.

The 1205 domains of the transformer are subdivided into eight (8) domain groups as shown in figure 4.7. In that figure 4.7, Air and core domains consist of single domains as before however winding domains were grouped at that stage as represented by their colors. Each phase has one primary and one secondary winding, these windings were further split into two groups because the geometry of the transformer is 2D and it is the

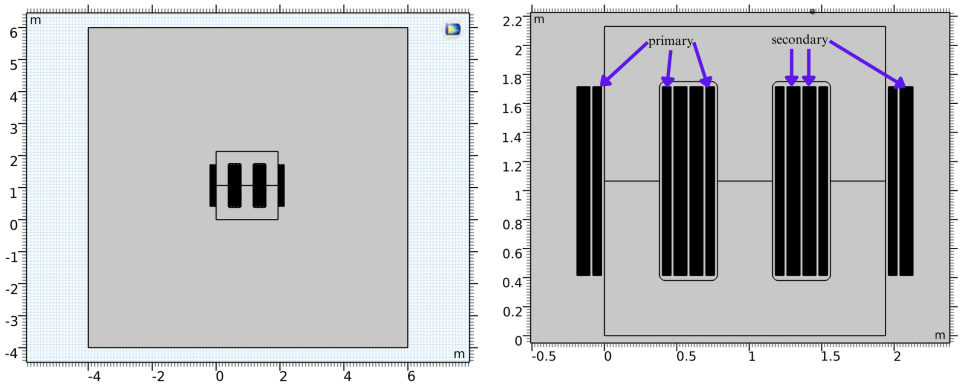

Figure 4.5: Whole 2D geometry of three phase transformer (a) and zoomed at core and windings (b)

Table 4.4: Geometry parameters of three phase transformer [5]

Description	**Value**	**Unit**
Thickness of core legs	380	*mm*
Air gap between core and primary windings	20	*mm*
Air gap between primary and secondary windings	20	*mm*
The thickness of single primary turn	1.3636	*mm*
Total thickness of primary windings	60	*mm*
The thickness of a single secondary turn	0.5769	*mm*
Total thickness of secondary windings	90	*mm*
Windings height (y-axis)	1370	*mm*
Height of the core (y-axis)	2130	*mm*
Core fillet radius	40	*mm*
Air gap between winding and core (y-axis)	50	*mm*
Number of turns in primary windings	44	−−
Number of turns in secondary windings	156	−−

way to define the direction of the current, In 3D geometry, it is one single round coil that is wounded throughout the leg of the core, hence this coupling can be avoided. There are 6 *Coil* domain groups in total including primary and secondary, and each *Coil* group has multiple domains that are connected in series (e.g., each Primary *Coil* has 44 domains that are connected in series together) [5].

The air and core domains are defined using *Ampere's law* domains from *Magnetic fields* physics. Air does not include hysteresis losses and uses linear relative permeability while the core domain was modeled with hysteresis losses and uses linear resistivity. The windings are described using *Coil* domains from *Magnetic fields* physics. Excitation current

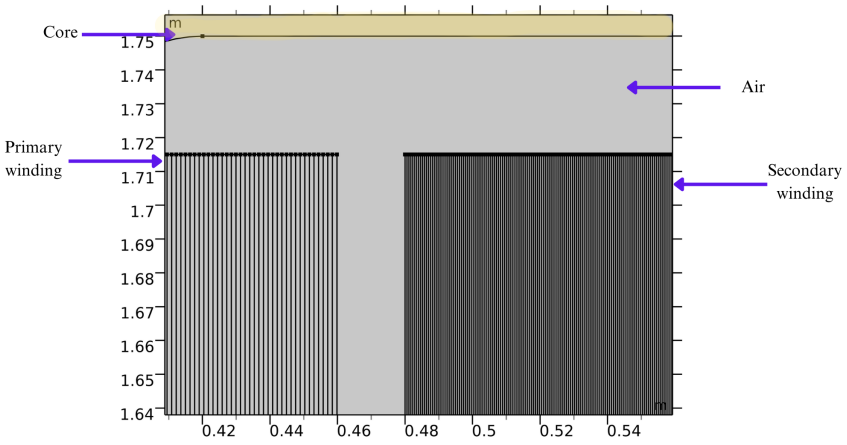

Figure 4.6: Zoomed at windings, 44 turns in primary and 156 in secondary

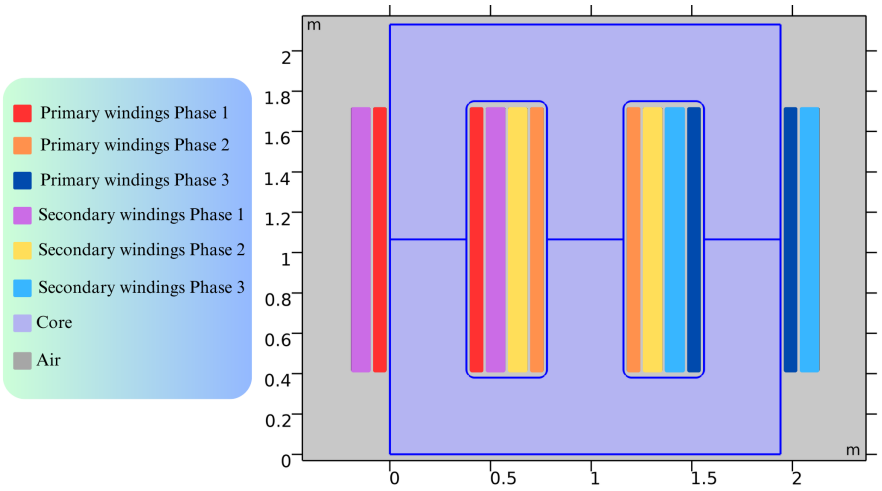

Figure 4.7: All eight (8) domain groups of Transformer

was linked with *Electric circuit* physics, by using the excitation option as external current (*IvsU*). The conductor was modeled as a single conductor and a coil group. If the coil group is selected, then reverse current can be defined by right click on the coil domain and choosing "Reverse current direction". The resulting current directions of all coils primary and secondary are shown in figure 4.8.

4.7 Material properties

Three materials are used from the Comsol material library:

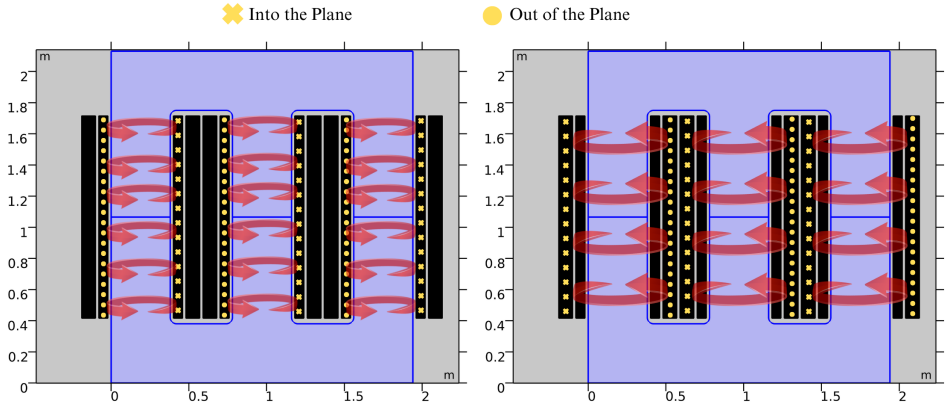

Figure 4.8: Direction of current in primary (a) and secondary coils (b)

Table 4.5: Material Properties

Property	**Symbol**	**Aluminum**	**Iron**	**Air**	**Unit**
Relative permittivity	ε_r	1	1	1	–
Heat capacity	C_p	900	444	Figure 4.9a	J/KgK
Thermal conductivity	k	238	74	Figure 4.9b	W/mK
Density	ρ	2700	7870	Figure 4.10a	Kg/m^3
Relative permeability	μ_r	1	1100+25j	1	––
Electrical conductivity	σ_e	Linear resistivity	Anisotopic	1	S/m
Dynamic viscosity	μ	–	–	4.10b	$Pa \cdot s$
Heat capacity ratio	γ	–	–	1.4	––

- Air
- Iron
- Aluminum

Properties of these three materials are given in table 4.5, where most of the properties are default however there are a few changes adopted in this thesis as presented in table 4.6.

To make the model stable with only one material property, the electrical conductivity (ρ_e) of air was changed from the default zero to one, as shown in table 4.6.

In table 4.6, linear resistivity (ρ_e), is used to include temperature dependency of electrical conductivity in aluminum, defined as an analytical function [5]:

$$\rho_e(T) = \rho_{e0}(1 + \alpha_T(T - T_{ref})) \tag{4.51}$$

Table 4.6: Changes in material properties

Domain	Property	Symbol	Default	New value	Unit
Air	Electrical conductivity	σ_e	0	1	S/m
Aluminum	Electrical conductivity	σ_e	3.774×10^7	$1/\rho_e$	S/m
Iron	Electrical conductivity	σ_e	1.12×10^7	σ_{Fe}	S/m
Iron	Relative permeability	μ_r	4000	$1100 + 25j$	$--$

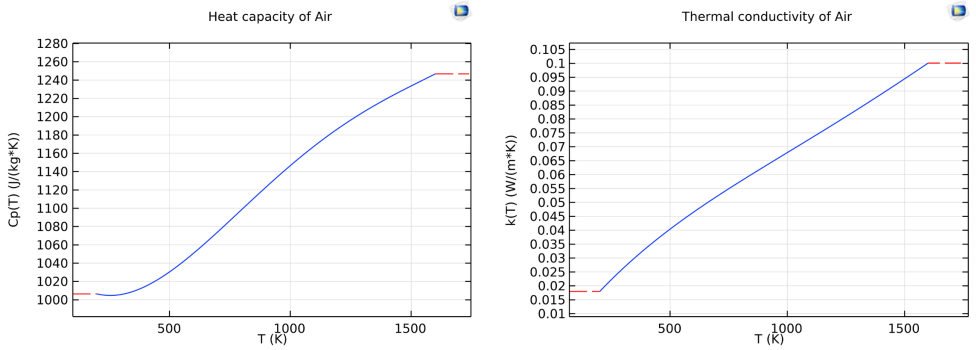

(a) (b)

Figure 4.9: Heat capacity (ε_r) of air (a), thermal conductivity (k) of air (b)

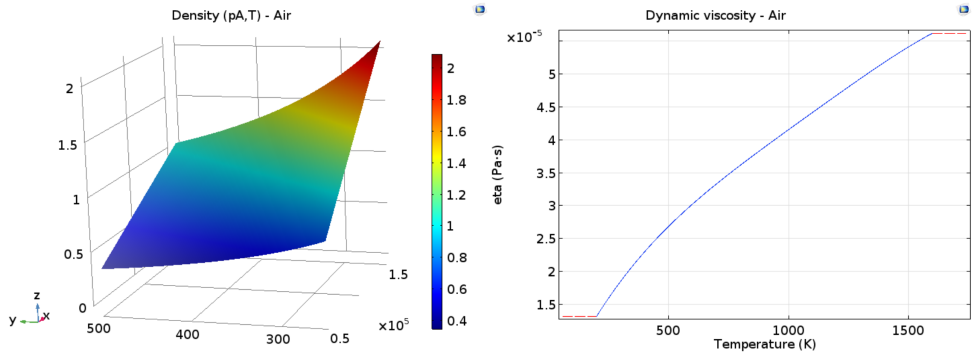

(a) (b)

Figure 4.10: Density (ρ) of air (a), dynamic viscosity (μ) of air (b), [5]

where:
$\rho_{e0} = 2.65 \times 10^{-8}$ resistivity at reference temperature, in (Ωm),
$T_{ref} = 20$ resistivity at reference temperature, in $(^\circ C)$,
$\alpha_T = 0.0039$ reference temperature, in $(^\circ C)$.

For iron, the electrical conductivity (ρ_e) was isotropic with a default value of $1.12 \times 10^7 S/m$, which means it has the same value for all directions. According to [5], it causes too much eddy current in the core, which induces a magnetic field opposite to induce a magnetic field of windings and results in the cancellation of the magnetic field of windings. Hence anisotropic electrical conductivity (σ_{Fe}) was presented which acts as lamination of the core and minimizes eddy currents of the core.

$$\sigma_{Fe} = \begin{bmatrix} 1.12 \times 10^7 & 0 & 0 \\ 0 & 1.12 \times 10^7 & 0 \\ 0 & 0 & 1 \end{bmatrix} \frac{S}{m}$$

In the above matrix, the conductivity of the core was changed from isotropic to anisotropic and it controls the conduction in the 3-dimensional axis. For instance, the matrix above (σ_{Fe}), conducts in the x and y direction but not in the z-direction and is given a value of $1 S/m$.

Another material property (μ_r) of the iron was changed from 4000 to 1100 just to make sure that the relative permeability of the core behaves in the linear region because transformers behave in the linear region. Imaginary part $25j$ of (μ_r) is used for including hysteresis losses[5].

Material properties that depend on temperature are defined in the Comsol material library as analytical functions and their graphs, heat capacity (ε_r) of air is given in figure 4.9(a), thermal conductivity (k) of air 4.9(b) and density (ρ) of air in figure 4.10(a), dynamic viscosity (μ) of air in presented in figure 4.10(b).

It should be noted that heat capacity ratio (γ) and dynamic viscosity (μ) are only required for modeling fluids in *laminar flow* physics. Iron and aluminum are solid at the modeling's expected temperature so it is not required, hence only air includes these properties in table 4.5.

4.8 Single phase transformer (model-2)

The single-phase 2D transformer model is a simplification of the three-phase transformer model presented earlier (model- 1) in figure 4.5. the geometry is almost identical to the three-phase model because it is extracted from the three-phase model, details are given in table 4.7. The overall geometry is shown in figure 4.11(a) while a closeup of a single phase transformer with details about coils is given in figure 4.11(b).

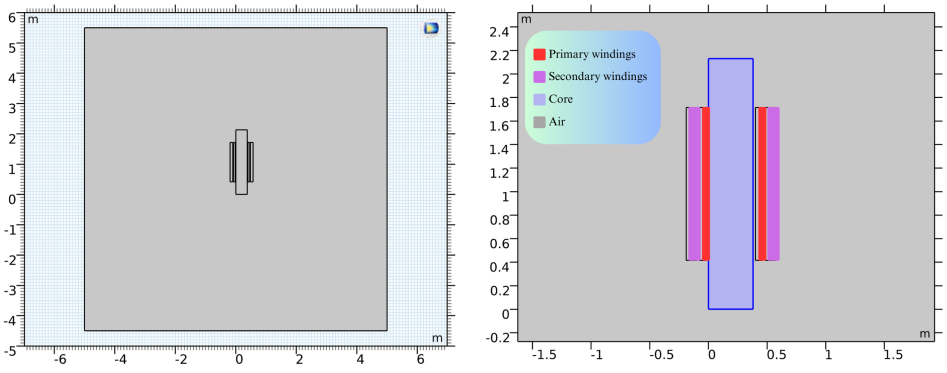

(a) (b)

Figure 4.11: Single phase (model-2) overall geometry (a), zoomed-in view with labeling (b),

Table 4.7: Geometry parameters of single phase transformer (model-1)

Description	**Value**	**Unit**
Thickness of core	380	*mm*
Air gap between core and primary windings	20	*mm*
Air gap between primary and secondary windings	20	*mm*
Total thickness of primary windings	60	*mm*
Total thickness of secondary windings	90	*mm*
Windings height (y-axis)	1370	*mm*
Height of the core (y-axis)	2130	*mm*
Number of turns in primary windings[1]	1	−−
Number of turns in secondary windings[2]	1	−−

The direction of the current in primary and secondary coils are shown in figure 4.12, where both primary and secondary coils consist of two coils that are grouped together. The direction of the coils can be assigned by choosing one of the domains from each group as the "reverse current direction".

Similar to the three-phase model, this model also uses the same physics with few changes in some parameters. Both models use 5 physics in total excluding multiphysics (for coupling two physics).

[1]At geometry stage, number of turns in the primary windings are modeled as a single piece of metal but at a later stage in the *Coil* domain, the primary coil will get a homogenized multiturn property, which behaves as a number of turns. The number of turns for the primary windings are 44.

[2]Similar to the primary domains, it is modeled as the single domain in the geometry but at a later stage in the *Coil* domain, the secondary coil will get a homogenized multiturn property too. The number of turns for the secondary windings are 156.

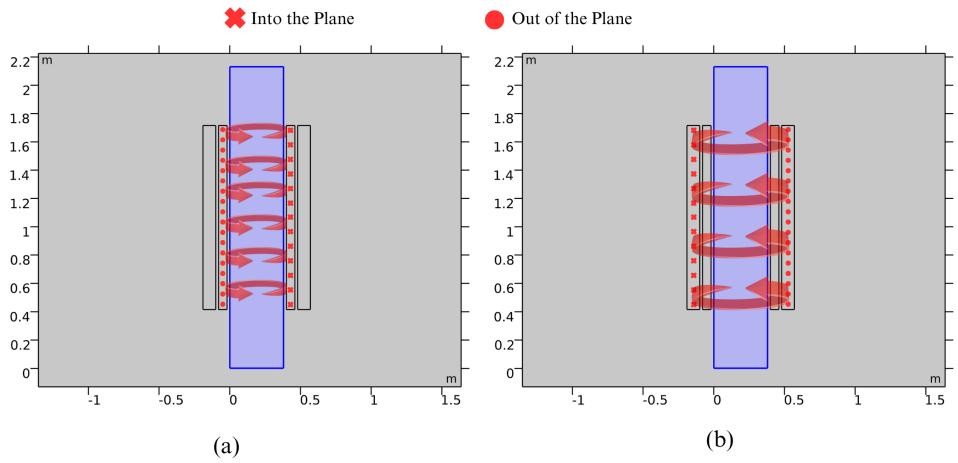

Figure 4.12: Direction of current in primary (a), and secondary coils (b)

- Magnetic fields
- Electrical circuit
- Heat transfer
- Laminar flow
- Surface-to-surface radiation

Air domain is modeled using *Ampere's law* domain from *Magnetic fields* physics, which does not include hysteresis loss while the core also uses *Ampere's law* domain but included hysteresis loss from magnetization model.

In electromagnetics, the coils are modeled using *Magnetic fields* physics, *Coil* domain. In this model-2, the coils are using conductor model as "homogenized multiturn" with 44 turns in primary and 156 in secondary, and excited through an external circuit *I vs U* coupling from *Electrical circuits*. The circuit diagram for *Electrical circuits* physics is shown in figure 4.13. The amplitude of voltage and currents for model-2 is the same as model-1 however there is an increase in primary current due to a change in core geometry and reluctance. *Heat transfer* and *Laminar flow* were the same, *Heat source* domain was modeled as a general source with "volumetric loss density" as input.

Since this model uses homogenized multiturn approximation for the modeling of coils, the model does not require huge computational costs and can run much faster however this comes at the cost of losing information about the skin and proximity effects in the coils which means there will be uniform current density which results in uniform heating in coils. Uniform heating in coils can predict the thermal analysis for overall temperature but is not good for hotspot analysis since all the windings behave as uniform current density instead of a real scenario where current density varies across the cross-section.

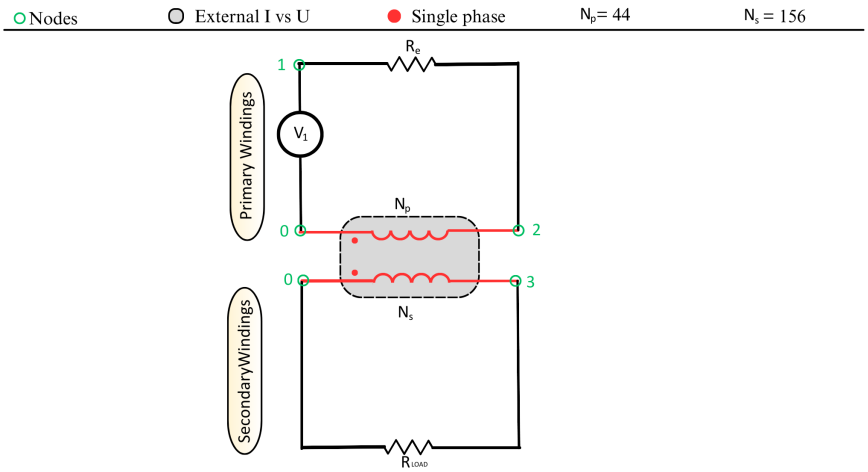

Figure 4.13: Single phase transformer circuit diagram (Model-2)

The model was solved in two studies. First, the electromagnetic study was solved which needs very small time steps to get a good resolution of transient analysis, only *Magnetic fields* and *Electrical circuits* physics were solved at this stage. Secondly, the stationary study was analyzed which has two steps, first Frequency domain was solved which solves the *Magnetic fields* and *Electrical circuits* physics by storing the solution of "Volumetric loss density" which would be used as input by the second step. In the frequency domain, hysteresis losses are included. In the second study step, the stationary study was solved for *Laminar flow*, *Surface to surface radiation*, and *Heat transfer in solids*. It should be noted that in time domain analysis, the "Voltage source" should be "Since source" which takes the frequency as input ($50Hz$) while for frequency domain analysis, the "Voltage source" should be "AC source" which does not take frequency as an input locally but it defined globally in the study.

5 Simulation Results

This chapter includes the simulation results from the analytical model and numerical modeling from COMSOL Multiphysics®. The sequence of the presentation of results is given below:

- Analytical model based on data from "Skagerak Energi".
- Three-phase numerical (FEM model 1) based on the data from "Agder Energi".
- Single phase Numerical (model-2), based on simplified data from [5].

In numerical modeling, the results of electromagnetic behavior are presented first, and later thermal modeling is presented for both models. Phases 1,2,3 are written as phases a, b, and c for primary and A, B, and C for secondary in Comsol to present primary and secondary voltages, currents, etc.

5.1 Analytic Model

The data from the power plants are sorted and converted into per-unit values as explained in Theory. The input data from the *Excel* file is displayed in *Julia* in figure 5.1. The main reason for choosing this data is because it has a good temperature rise from start to steady state.

For this simulation, the epochs were 8000 which is enough since the error does not go further down after more iterations as shown in figure 5.2, and the minimum error (losses) in the approximation was 127.37. This may go even further if there weren't any minor discontinuities in the data (CSV).

The approximation data is shown in figure 5.3 using basic thermal equations. The graph shows good estimations.

The thermal resistance of the oil $R_{,}th_oil = 52.32K/W$ is estimated using the neural network in *julia.* and the thermal time constant $\tau_{oil} = 111mins$. This estimation seems reasonable. The model was verified using the copper losses calculation presented earlier and the results were almost the same where the time constant found was $\tau_{oil} = 112mins$.

This estimation is used as an input to the modified IEEE method.

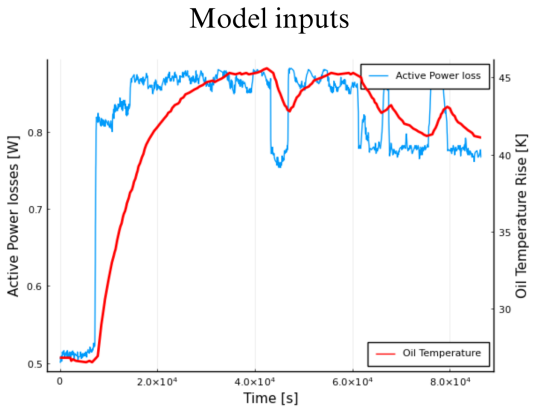

Figure 5.1: Inputs data for the analytical model from *Skagerak*

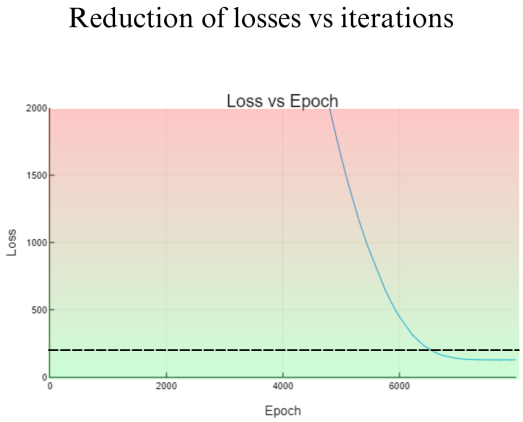

Figure 5.2: Error reduction using flux package in *Julia*

The temperature estimation using the IEEE method for top oil is shown in figure 5.4 where this temperature becomes the input for the hotspot temperature estimation in figure 5.5, and finally figure 5.6 shows the hotspot temperature variation for under load, rated load and overload. It is important to note that the time scale for all plots is not the same, for better visualization, scales are modified.

5.2 Three phase transformer (FEM model 1)

The voltage from the primary and secondary windings of the transformer is shown in figure 5.7, where the transformer is operating at full load. The load resistance is $R_{load} = 105.8\Omega$.

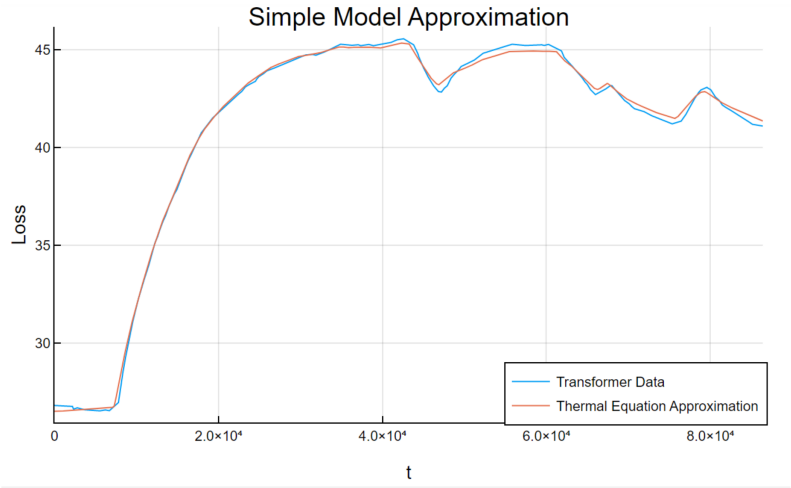

Figure 5.3: Approximated data vs the original data using *Julia*

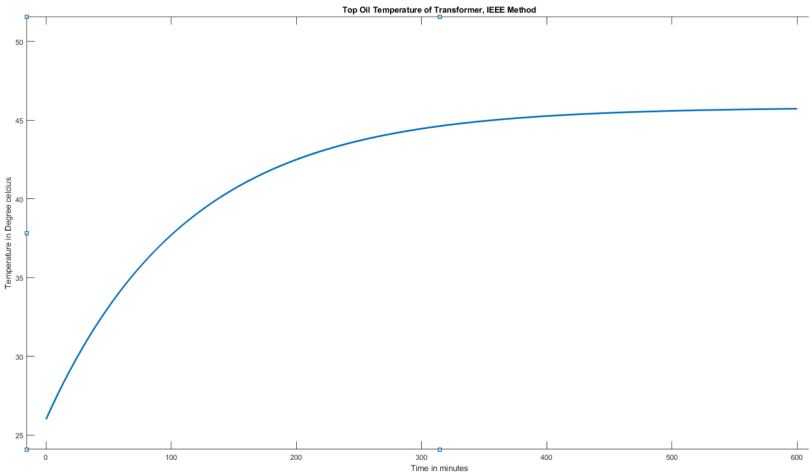

Figure 5.4: Top Oil temperature using modified IEEE *Matlab*

The circuit of the transformer is shown in figure 4.4. The input primary voltage has a phase difference of 120° as presented in table 4.3.

The current from the primary and secondary windings of the transformer is shown in figure 5.8, at maximum capacity. Current in the primary windings is higher than the secondary since it is a setup transformer. Both, voltages and current plots show that the transformer is working stable. If the load resistance is decreased too much (increasing load beyond the capacity) then the transformer goes out of balance.

Since this model is very complex as it has more than 1200 domains, every single turn of the coil has its own geometry as shown in figure 4.6, therefore skin and proximity effects can be seen in the windings in figure 5.9. The current density in the whole transformer

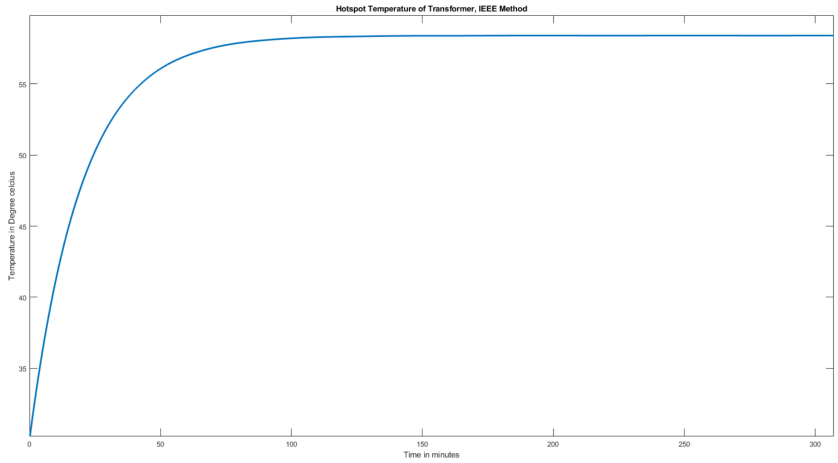

Figure 5.5: Hotspot temperature estimation using modified IEEE *Matlab*

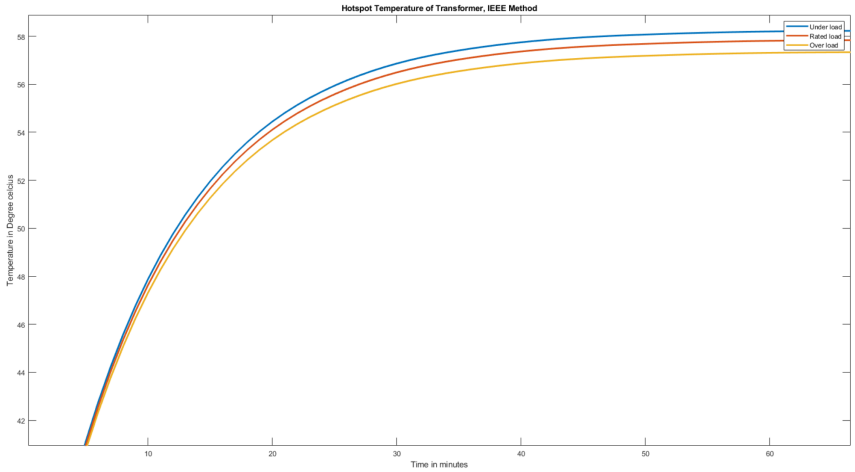

Figure 5.6: Hotspot temperature estimation at under load, rated load and overload using modified IEEE *Matlab*

is too small as compared to the corners of the windings, both bottom and top edges of windings, this is due to skin and proximity effects. Boundary edges are not modeled for better visual graphs because of the very detailed geometry of windings. A zoom-in view of the top right corner, for a better visual of current density, is shown in figure 5.9(b),.

Eddy currents in the core are shown in figure 5.10, only the core domain is selected in the surface plot, outer edges have almost zero or very less eddy current however current density is highest in the middle leg due to the stronger magnetic field in that closed region surrounded by coils on both sides, which induce higher eddy currents.

Hysteresis losses in the overall core are shown in figure 5.11(a), and zoomed-in at the edges

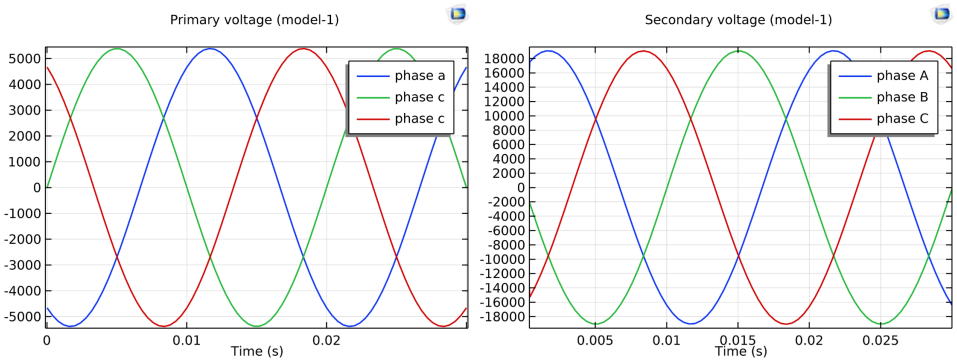

(a) (b)

Figure 5.7: Three phase transformer (model-1) primary (a), and secondary voltage (b)

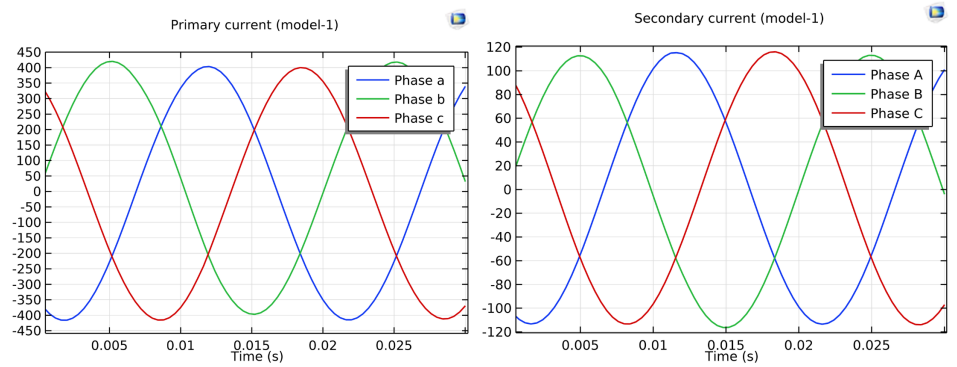

(a) (b)

Figure 5.8: Three phase transformer (model-1) primary (a), and secondary current (b)

of the core is shown in (b). Hysteresis losses peak at the corners, with the maximum value of $21.1 kW/m^3$ The core is having a corner radius of (40mm) as given in the geometry table 4.4. Only the core domain from *Magnetic fields* includes modeling of hysteresis losses, the imaginary part of the relative permeability ($25j$) results in hysteresis losses in the core, complete details of the parameters can be found in table 4.5.

Flux density in the core is shown in figure 5.12, where the electrical conductivity is anisotropic which means the core conducts in both the x and y-axis but not in the z-axis, reason and details for this is found in section 4.7. If isotropic (default) electrical conductivity would be used, it will end up with no overall magnetic flux in the core, due to the non-laminated behavior of the core. The highest flux density in the core is $2.86T$ and the average flux density is $1.1T$.

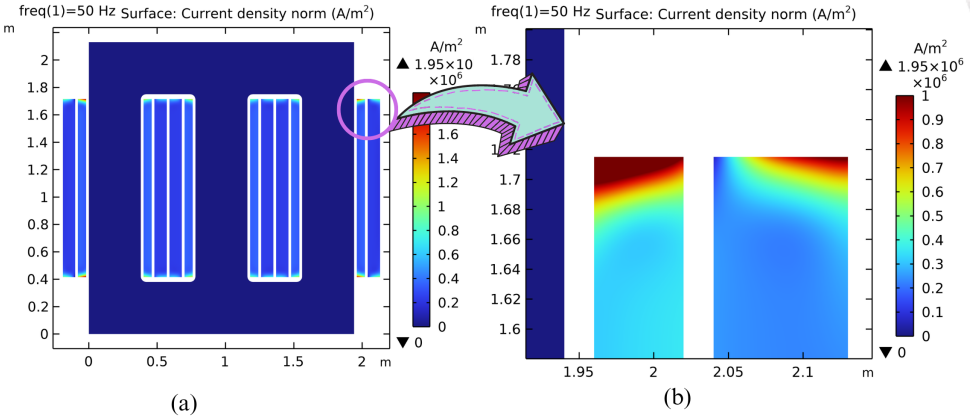

Figure 5.9: Current density (model-1) (a), and zoomed at corners (b)

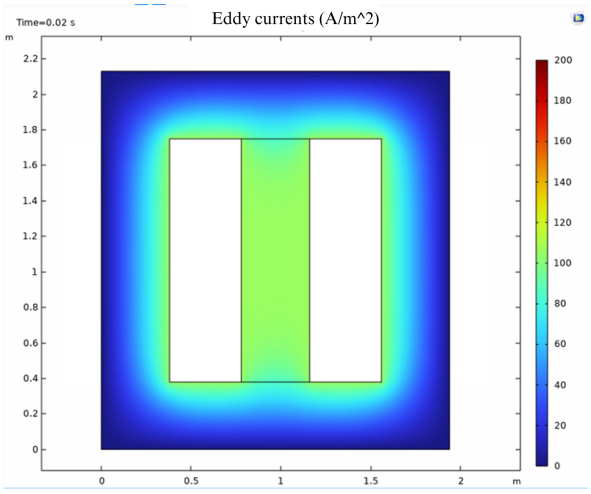

Figure 5.10: Eddy current in iron core (model-1)

5.2.1 Homogenized approximation coils (model-1)

The geometry of the *Coil* domain in the previous electromagnetic analysis was very detailed and it consists of 1200 domains, which required very detailed mesh and high computational powers. The electromagnetic analysis presented in the previous section was based on time-dependent analysis and frequency domain analysis which have transient behavior however for the thermal analysis, the rate of temperature rise is very slow as compared to changes in voltage, frequency, currents, etc. To run the small simulations based on around 100 steps, *Comsol* easily takes hours to finish it without including heat physics in the solver, otherwise this time reaches days. One attempt was done to reduce the resolution of the study, by increasing the step size, but the model becomes unstable

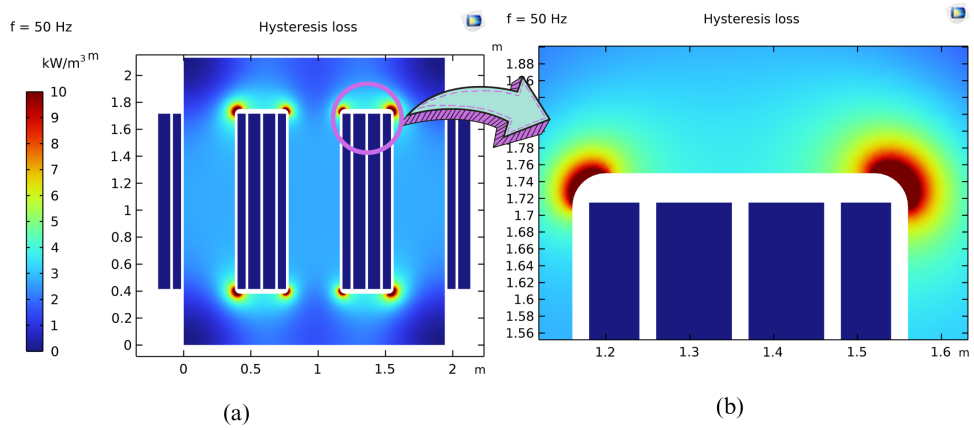

Figure 5.11: Hysteresis losses in core overall (model-1)(a), zoom into the corner of the core (b)

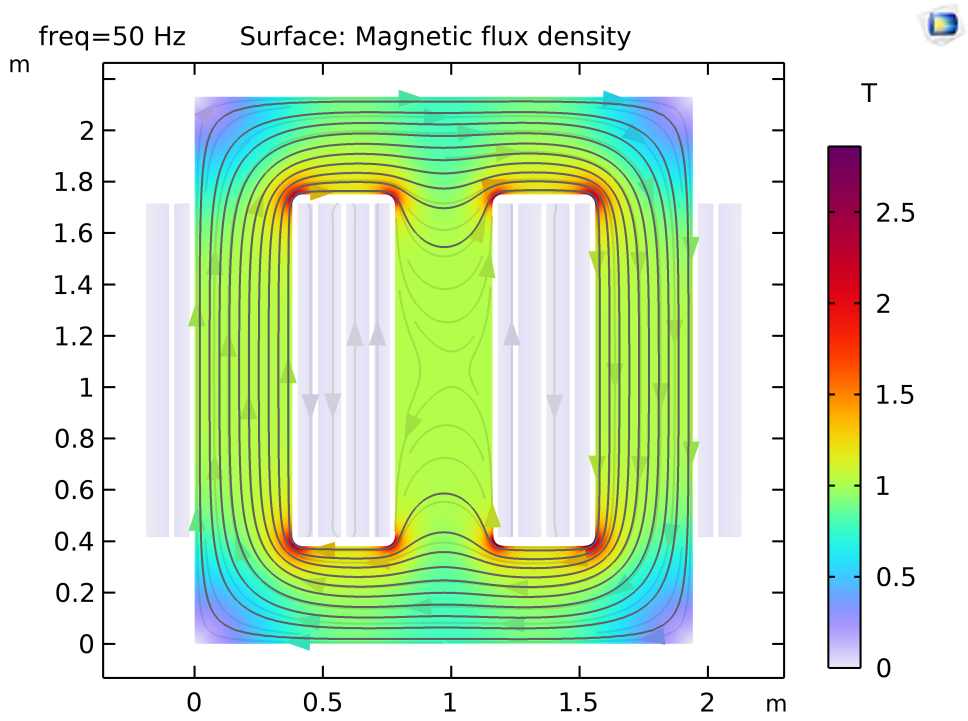

Figure 5.12: Magnetic flux density (model-1) with anisotropic electrical conductivity

after continuously running for 2 days and 14 hours because electromagnetic and heat domains are opposite in time frames. To cope with this problem there are a few steps taken after spending time with *Comsol*:

- The geometry of the *Coils* changed from 1200 highly detailed to just 12 domains.

Only one geometry for the whole coil.

- It is not feasible to run both *electromagnetic* study and *Thermal analysis* in the same solution as both require very opposite time steps.

Two changes bring two challenges for the analysis:

- If *Coils* are modeled as single conductor geometry and their number of turns are defined from then *Magnetic field* physics, then the *Coil* model is considered as *homogenized muliturn* which uses an approximation of coils but this way of defining *Coils* can not include "skin effect" and "proximity effect" in the *Coils*, which results in uniform current density, which means uniform losses, that ends up in uniform heating throughout the coil, and hence *hotspot* analysis cannot be modeled however thermal analysis can be modeled using this.

- There was a challenge, If two types of studies are solved separately, there must be a system to couple them, *electromagnetic* losses must be coupled from the first physics and used as input for the thermal analysis.

Three phase transformer (model-1) with simplified geometry is shown in figure 5.13, where 1200 domains are simplified into six single conductor domains. It looks similar to the detailed geometry model when looked from far away figure 4.5 however if zoomed in at the windings, the comparison between the non-homogenized (model-1) in figure 5.14 (left) can be more visible and obvious with homogenized (model-1) in figure 5.14 (right).

When three-phase transformer model-1 was rebuilt using homogenized *Coil* configuration, there were no skin and proximity effects in the coils, hence electromagnetic losses and current density was uniformly distributed throughout the coils. This is better illustrated in one of the comparison figures 5.15, where the primary coil of phase 1 was taken as a reference and zoomed in to it before homogenized approximation and after homogenized approximation. It should be noted that both models are built separately from scratch, it's not a duplicate copy of the first model, hence the comparison is mainly to show the distribution of losses throughout the geometry rather than numbers.

For thermal analysis of the model-1 which has homogenized coils at this stage, two study steps for temperature. First, the frequency domain study was analyzed and electromagnetic losses are stored in the solver which then become the input for the second stationary study results of the heat transfer are shown in figure 5.16. The ambient temperature was $20°C$ and Laminar flow was used for fluid domain analysis however the fans are turned off (very low 0.04 m/s natural air flow) but gravity is included in the model. Hot lighter air is moving upward and surface-to-surface radiation is included in the model. The temperature peaks around $110°C$ in primary windings at maximum loading also note that this model includes the temperature-dependent resistivity in the windings, if that is not included then the temperature should be a little lower.

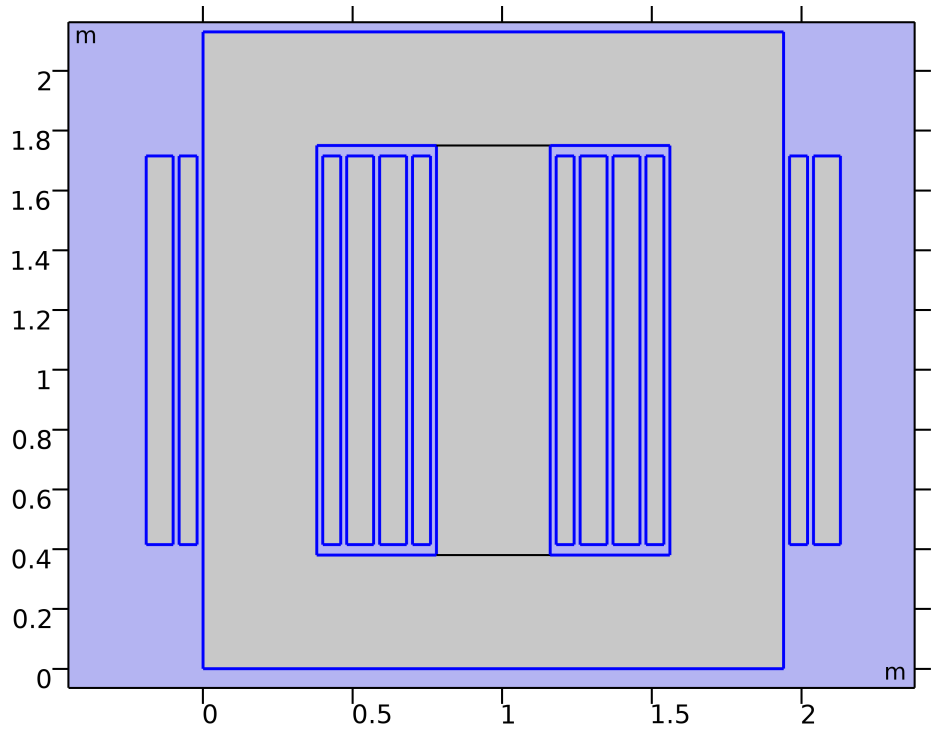

Figure 5.13: Three phase transformer (model-1) with homogenized coils

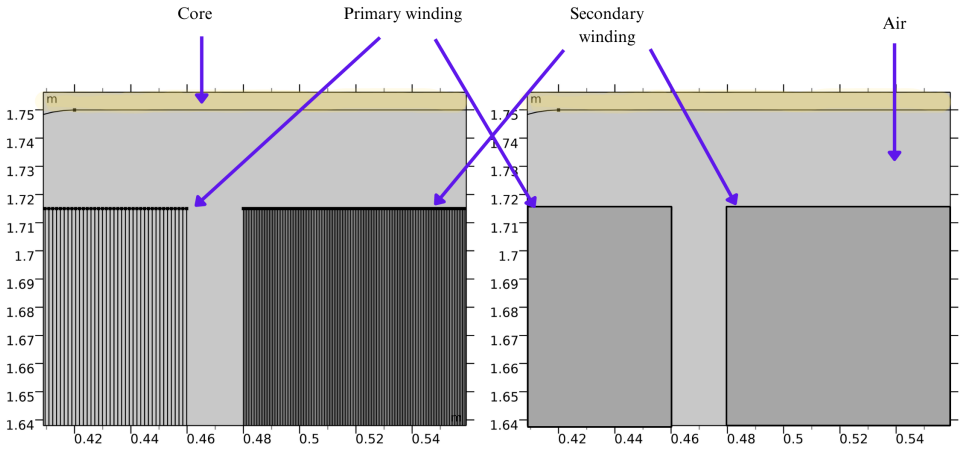

Figure 5.14: Three phase transformer geometry zoomed in (model-1), non-homogenized (left) vs homogenized (right)

Since homogenized coils are used, results are only approximations for thermal stress but we can not see the hotspots or the location in geometry.

The velocity of the air can be seen in figure 5.17 which is given a value of 0.04 just for the natural air flow from the surrounding. This is modeled in *Laminar Flow*

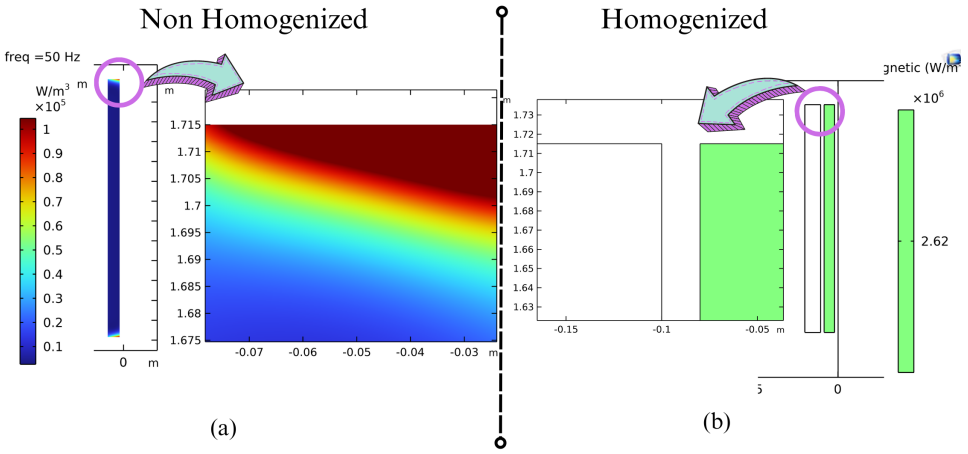

Figure 5.15: Effects of homogenized coils on electromagnetic losses in coils, before (a) and after (b)

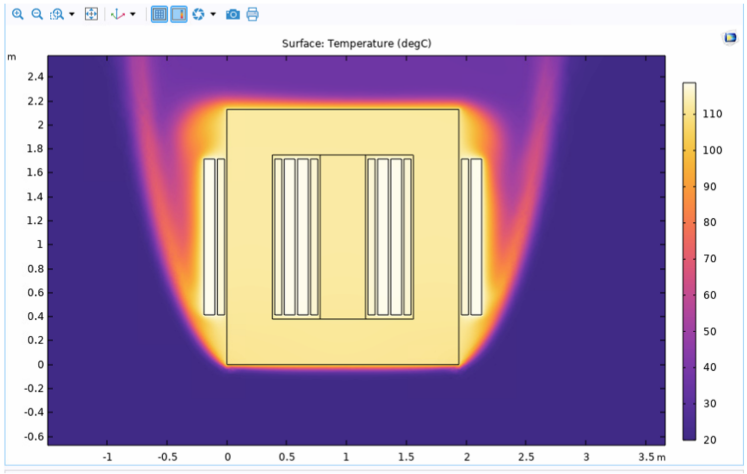

Figure 5.16: Steady state temperature of Three-phase transformer (model-1)

5.2.2 Future models

Some models that I used in this section of the thesis will be used in the presentation but not part of the (written) thesis because of the very limited time of the thesis. However few figures are attached below 5.18, 5.19.

A comparison between model-1 and model-2 is shown in figure 5.20, where model-1 is the main three-phase model and model-2 is the most simplified model. Unfortunately, I ran out of time to explain that model in this thesis. Model-1 is based on the data from table 4.4 and model-2 from table 4.7.

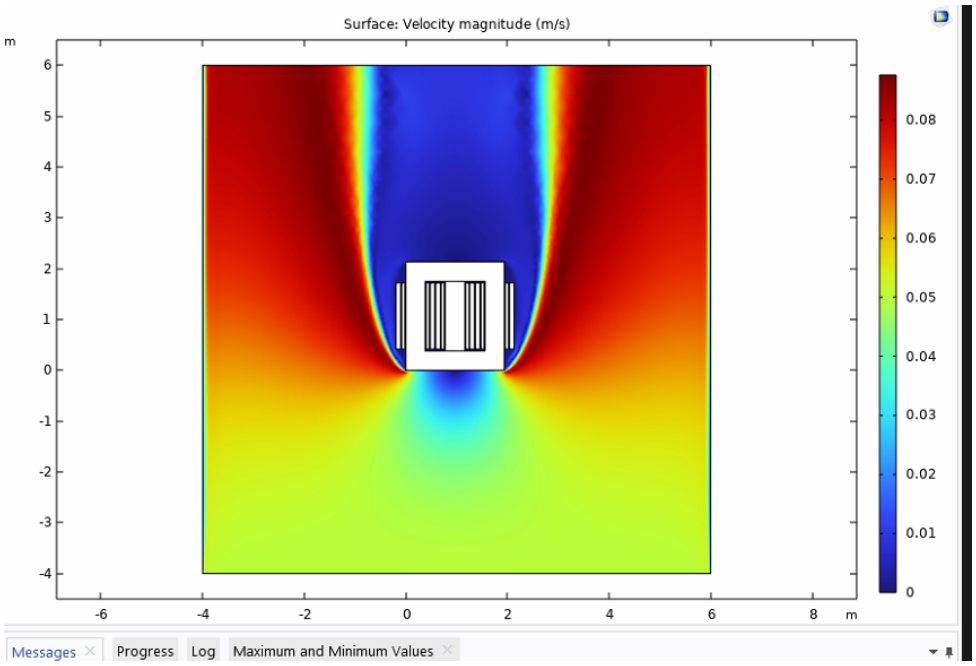

Figure 5.17: Velocity of the air (model-1)

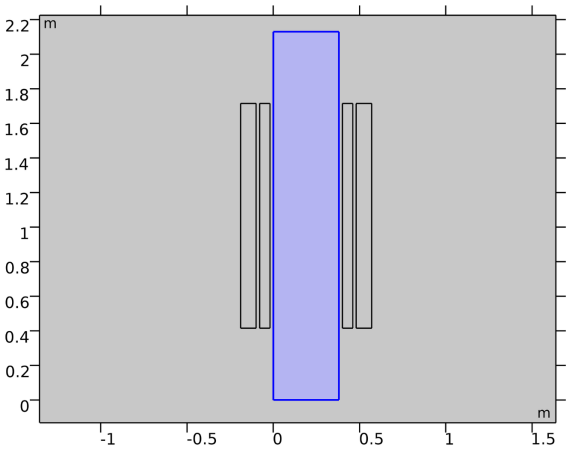

Figure 5.18: Singel phase model based on the data three-phase (model-2)

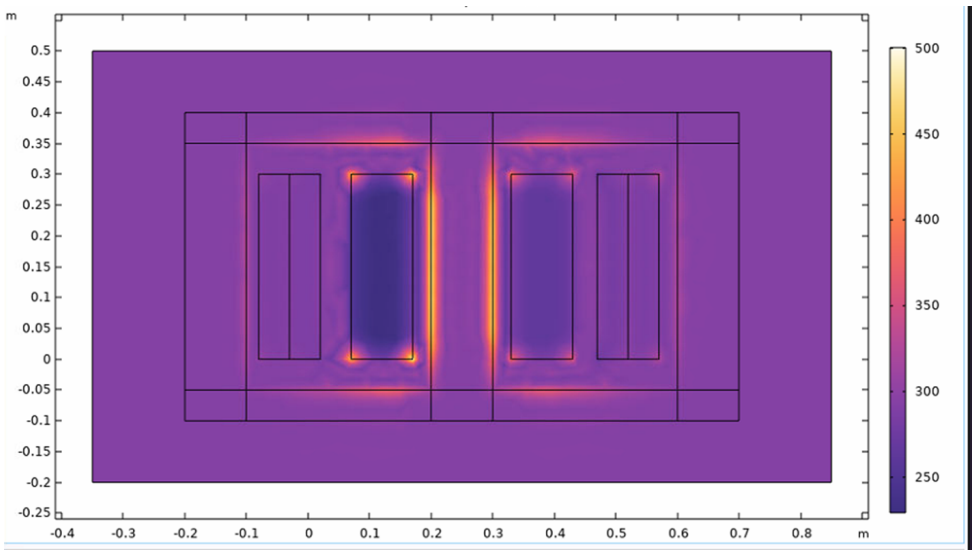

Figure 5.19: Another thermal test model, for future (model-3)

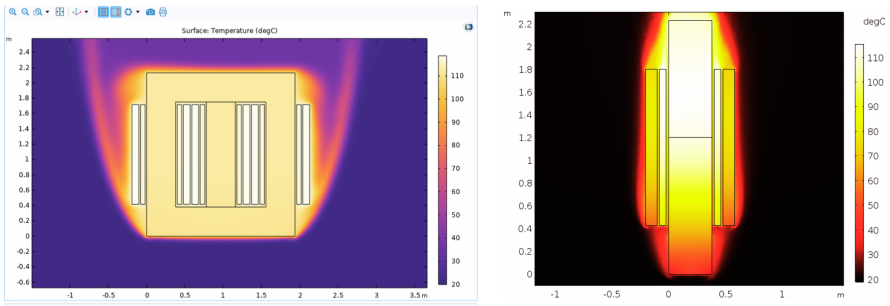

(a) (b)

Figure 5.20: Comparison of three phase model heat run steady state (a) vs single phase (b)

6 Discussions

In this thesis, two types of approaches are used to analyze the behavior of the transformers when they are overloaded or thermal stress when they are approaching maximum limits.

- Analytical lumped model
- Numerical modeling using Comsol

In Analytical modeling, the data was provided from the Skagerak based on the real transformer, however, data was very limited, but with the help of the neural network, time constants are estimated and later modified IEEE methods are used to analyze the hotspot temperature.

In Numerical modeling, two types of analyses are performed:

- Electromagnetic
- Thermal

Electromagnetic analysis was successfully conducted on a dry-type three-phase transformer with multiple single-turn coils to describe windings. Skin effects and proximity effects are explained in the simulations. Current density and hysteresis losses are also explained.

Thermal modeling required a very big time to simulate with electromagnetic modeling however, homogenized approximations are used to speed up the analysis. Skin depth and proximity effects are excluded from the models using the approximations and hence, hotspots can not be estimated however thermal analysis was finished on three-phase transformer model-1, where the highest temperature in the windings was observed around 110 degrees with out external coolings.

7 Conclusion and future work

I have a few suggestions:

- Building two non-homogenized models and extracting the magnetic losses data from the first model and using it to give as input to the homogenized model that has exactly the same geometry. That data must have a relationship of current density along with geometry.
- The three-phase model can be simulated in 3D instead of 2D.
- Building the thermal model based on the data from Hitachi Energy and comparing the results.
- For analytical modeling, this model can be tested on a physical transformer that has fiber optic probes for measurement of the hotspot temperatures so data can be cross-verified.

References

[1] W. H. Tang and Q. H. Wu, *Condition monitoring and assessment of power transformers using computational intelligence*. Springer Science & Business Media, 2011.

[2] D. Susa, M. Lehtonen and H. Nordman, 'Dynamic thermal modelling of power transformers,' *IEEE transactions on Power Delivery*, vol. 20, no. 1, pp. 197–204, 2005.

[3] N. Patel and P. Shah, 'Thermal modelling of power transformers,' *International Journal of Engineering Development and Research*, 2014.

[4] E. E. Agency, 'Share of energy consumption from renewable sources in europe,' *Online Article*, 2022.

[5] S. Attestog, 'Electromagnetic and thermal modelling for prognosis of distribution transformer,' M.S. thesis, Universitetet i Agder; University of Agder, 2018.

[6] H. Stewart and L. Whitman, 'Hot-spot temperatures in dry-type transformer windings,' *Electrical Engineering*, vol. 63, no. 10, pp. 763–768, 1944.

[7] S. Chakravorti, D. Dey and B. Chatterjee, 'Recent trends in the condition monitoring of transformers,' *Power Systems Springer-Verlag: London, UK*, 2013.

[8] electrical4u.com, 'Dry-type transformer,' *Online Article*, 2018.

[9] 'Dry-type transformers,' *IEC 60076-11:2004 Power transformers, IEC, 2004, p. 75.*, 2004.

[10] H. E. P. Transformer, 'Oil-immersed transformer definition, composition, and design features,' *Online Article*, accessed 03-April-2023.

[11] 'Liquid-filled power transformers,' *available at : https://library.e.abb.com/public/299a52373cfd0e6c12578be003a476f/PPTR$_M$PT$_b$rochure$_2$406L170−W1−en.pdf*, online accessed: April 2023.

[12] D. Belefic, 'Oil filled transformer,' *Online Article*, accessed 03-April-2023.

[13] D. Transformer, 'What is the structure of the oil immersed transformer?' *Online Article*, accessed 03-April-2023.

[14] elprocus.com, 'What is three-phase transformer : Construction and its working,' *Online Article*, accessed 03-April-2023.

[15] Tameson.com, 'Three-phase transformers: A comprehensive guide,' *Online Article*, accessed 03-April-2023.

[16] S. Mousavi, 'Electromagnetic modelling of power transformers for study and mitigation of effects of gics,' Ph.D. dissertation, KTH Royal Institute of Technology, Stockholm, Sweden., 2015.

[17] S. V. Kulkarni and S. A. Khaparde, *Transformer engineering: design, technology, and diagnostics*. CRC press, 2017.

[18] B. Reclamation, 'Transformers: Basics, maintenance and diagnostics,' *US Department of the Interior Bureau of Reclamation. Denver, Colorado, USA*, 2005.

[19] C. W. T. McLyman, *Transformer and inductor design handbook*. CRC press, 2004.

[20] Allumiax, 'Difference between core form and shell form power transformers,' *available at : https://www.allumiax.com/difference-between-core-form-and -shell-form-power-transformers-by-generalpac*, accessed 2023.

[21] Cara, 'Everything you need to know about transformer cores,' *Online Article*, accessed 03-April-2023.

[22] M. Heathcote, *J & P Transformer Book*. Elsevier Science, 2011.

[23] A. Skillen, A. Revell, H. Iacovides and W. Wu, 'Numerical prediction of local hot-spot phenomena in transformer windings,' *Applied Thermal Engineering*, vol. 36, pp. 96–105, 2012.

[24] elprocus.com, 'What is transformer winding : Types and its applications,' *Online Article*, Online; accessed 03-April-2023.

[25] K. Banerjee, 'Transformer tap: What, why, how to find and detailed facts,' *Online Article*, accessed April,2023.

[26] M. Transformers, 'Why are transformer insulation system ratings important?' *Online Article*, accessed April,2023.

[27] L. L. Grigsby, *The electric power engineering handbook-five volume set*. CRC press, 2018.

[28] M. K. Saini. 'Cooling methods of a transformer.' (Accessed: May 05, 2023), [Online]. Available: `https://www.tutorialspoint.com/cooling-methods-of-a-transformer`.

[29] Electrical4u, 'Transformer cooling system and methods,' Accessed: May 05, 2023. [Online]. Available: `https://www.electrical4u.com/transformer-cooling-system-and-methods/https://www.tutorialspoint.com/cooling-methods-of-a-transformer`.

[30] M. kumar Saini, 'Difference between single-phase and three-phase transformer,' *Online Article*, 2022.

[31] S. J. Chapman, *Electric Machinery Fundamental*. WCB/McGraw-Hill, 2011.

[32] Allumiax, 'Hysteresis,' *available at : https://https://byjus.com/jee/hysteresis/*, accessed May, 2023.

[33] A. Roderick. 'Transformer losses and efficiency.' (Accessed: May 04, 2023), [Online]. Available: https://eepower.com/technical-articles/transformer-losses-and-efficiency/#.

[34] 'Types of losses in a transformer.' (Accessed: May 04, 2023), [Online]. Available: https://circuitglobe.com/types-of-losses-in-transformer.html.

[35] R. W. Hurst. 'Transformer losses explained.' (Accessed: May 04, 2023), [Online]. Available: https://www.electricityforum.com/iep/electrical-transformers/transformer-losses.

[36] Pratik. 'Free convection vs forced convection.' (Accessed: May 05, 2023), [Online]. Available: https://mechcontent.com/free-convection-vs-forced-convection/.

[37] W. McNutt, J. McIver, G. Leibinger, D. Fallon and K. Wickersheim, 'Direct measurement of transformer winding hot spot temperature,' *IEEE transactions on power apparatus and systems*, no. 6, pp. 1155–1162, 1984.

[38] J. Declercq and W. Van Der Veken, 'Accurate hot spot modeling in a power transformer leading to improved design and performance,' in *1999 IEEE transmission and distribution conference (Cat. No. 99CH36333)*, IEEE, vol. 2, 1999, pp. 920–924.

[39] M. T. Isha and Z. Wang, 'Transformer hotspot temperature calculation using ieee loading guide,' in *2008 International Conference on Condition Monitoring and Diagnosis*, IEEE, 2008, pp. 1017–1020.

[40] A. L. Ribeiro, N. Eira, J. Sousa, P. Guerreiro and J. Salcedo, 'Multi-point fibre optic hot-spot network integrated into a high power transformer,' in *Third European Workshop on Optical Fibre Sensors*, SPIE, vol. 6619, 2007, pp. 612–615.

[41] M. Lee, H. A. Abdullah, J. C. Jofriet and D. Patel, 'Temperature distribution in foil winding for ventilated dry-type power transformers,' *Electric Power Systems Research*, vol. 80, no. 9, pp. 1065–1073, 2010.

[42] X. Ding and W. Ning, 'Analysis of the dry-type transformer temperature field based on fluid-solid coupling,' in *2012 Second International Conference on Instrumentation, Measurement, Computer, Communication and Control*, IEEE, 2012, pp. 520–523.

[43] M. Arjona, C. Hernandez, R. Escarela-Perez and E. Melgoza, 'Thermal analysis of a dry-type distribution power transformer using fea,' in *2014 International Conference on Electrical Machines (ICEM)*, IEEE, 2014, pp. 2270–2274.

[44] D. Susa, 'Dynamic thermal modelling of power transformers,' Ph.D. dissertation, Helsinki University of Technology, FINLAND, 2005.

[45] A. Germanov, 'Deep learning with julia – how to build and train a model using a neural network,' Accessed: May 14, 2023. [Online]. Available: https://dev.to/andreygermanov/deep-learning-with-julia-how-to-build-and-train-a-model-using-a-neural-network-40pe.

[46] H. Xiaofeng, Z. Lijun, W. Guangning and D. Qingquan, 'Simulation models of transformer hot-spot temperature,' in *2012 IEEE 10th International Conference on the Properties and Applications of Dielectric Materials*, 2012, pp. 1–4. DOI: 10.1109/ICPADM.2012.6318943.

[47] C. Multyphysics. 'Comsol multiphysics quick start and quick reference v5.5.' (Accessed: April 10, 2023), [Online]. Available: https://doc.comsol.com/5.5/doc/com.comsol.help.comsol/comsol_ref_equationbased.23.008.html.

[48] R. A. Adams and C. Essex, *Calculus: A Complete Course, with My Matlab*. Pearson, 2013.

[49] C. Jaewook, 'Modelling and simulation of a power transformer using numerical thermal analysis,' M.S. thesis, Tallinn University of technology, 2019.

Appendix A

Derivation of formula for number of turns

According to Faraday's law of electromagnetism whenever a conductor is placed in the vicinity of changing magnetic fields, an electromotive force is induced.

$$V = -N \cdot \frac{d\phi_B}{dt} \tag{A.1}$$

where:

V = voltage,
ϕ_B = induced magnetic flux.

Using equation A.1, applying known voltage V, the number of turns in primary and secondary windings can be calculated. In transformers, magnetic flux ϕ_B depends on the product of flux density B and the cross-sectional area surrounded by the coil A_{coil} but it is assumed that the core is the main conductor, hence the cross-sectional area of the core A_{core} is used instead [5].

$$\phi_B = A_{core} \cdot B \tag{A.2}$$

Substituting ϕ_B from equation A.2 to equation A.1 becomes:

$$V = -N \cdot A_{core} \cdot \frac{dB}{dt} \tag{A.3}$$

The sinusoidal voltage signal is defined by:

$$V = \sqrt{2} \cdot V_{RMS} \cdot \sin(2\pi f t) \tag{A.4}$$

where:
V_{RMS} = Root Mean Square voltage,

f = frequency,
t = time period.

In equation A.4, $V_{RMS} = 0.7071 * V_p$ and V_p = peak voltage.

Substituting equation A.4 in equation A.3 becomes:

$$\sqrt{2} \cdot V_{RMS} \cdot \sin(2\pi ft) = -N \cdot A_{core} \cdot \frac{dB}{dt} \tag{A.5}$$

Integrating both sides of equation A.5 gives:

$$\sqrt{2} \cdot V_{RMS} \cdot \int \sin(2\pi ft) dt = -N \cdot A_{core} \cdot \int B(t) dt \tag{A.6}$$

$$-\frac{\sqrt{2} \cdot V_{RMS} \cdot \cos(2\pi ft)}{(2\pi f)} = -N \cdot A_{core} \cdot B(t) \tag{A.7}$$

Flux density B(t) is maximum when $cos(x)$ is maximum e.g., $cos(2\pi) = 1$, equation A.7 at maximum flux density becomes :

$$\frac{V_{RMS} \cdot t}{(\sqrt{2}\pi)} = N \cdot A_{core} \cdot B_{max} \tag{A.8}$$

Equation A.8 for calculating number of turns becomes:

$$N = \frac{\sqrt{2} \cdot V_{RMS}}{2\pi \cdot B_{max} \cdot A_{core} \cdot f} \tag{A.9}$$

Appendix B

Task description

A signed description of the task for this thesis is available on the next page.

University of
South-Eastern Norway

Faculty of Technology, Natural Sciences and Maritime Sciences, Campus Porsgrunn

FMH606 Master's Thesis

Title: Modeling of hot-spots in transformer (or the excitation system) using analytical or numerical methods (2D FE – COMSOL or Similar)

USN supervisor: Thomas Øyvang, Dany Tome, Frederic Maurer

External partner: Skagerak Kraft, SysOpt Project

Task background:
This project is located in the complex "SysOpt", more specifically within the working package about "boosting" of the hydro-generator. The boosting mode of the hydro-generator means to produce "much more" (Q>1p.u.) reactive power during a short time period (2' up to few hours until it reaches thermal equilibrium) to ensure grid stability, within a context of renewable power penetration into the electrical grid and high electrification leading to higher power variation. There are several ongoing works in this work package and this master thesis will focus on two components that are not covered yet: the main transformer and the excitation. When going into the boosting mode, the generator will produce much more reactive power than in nominal conditions, therefore it must be ensured that the excitation system and the main transformer can withstand this operation mode without any damage. Despite higher electro-magnetical forces that could occur in case of short-circuit, higher thermal loading of the components has been identified as the major risks/problems associated with this special operating mode.

The major goal of this thesis is to enhance the knowledge about the thermal impact on the main transformer and excitation system of the boosting operation mode.

Task description:

Following is a list of tasks to be performed to analyse the cooling / losses of a main transformer or excitation system, provide a computation model and try to provide some guidelines to extend the boosting operation mode of this components.

1. Analyse a 3-phase main transformer / excitation system
2. Analyse the cooling methods of this components and chose on type for deeper study
3. Analyse the used loss models in the literature
4. Establish a computation method (analytical and / or numerical) to model the main transformer / excitation system from a loss / cooling perspective
5. Cross-check this model against measured quantities (for example at rated operation mode)
6. Compute expected temperature rise at boosting operation mode and define a boosting mode operation range
7. Provide some guidances about problems and potential solutions to extend the boosting operation range.

Student category: EPE

Is the task suitable for online students (not present at the campus)? Yes

Practical arrangements: NA

Supervision:

As a general rule, the student is entitled to 15-20 hours of supervision. This includes necessary time for the supervisor to prepare for supervision meetings (reading material to be discussed, etc).

Signatures:

Thomas Gyrong 05.02.23

Supervisor (date and signature):

MUHAMMAD MUNEEB

Student (write clearly in all capitalized letters):

03/02/23

Student (date and signature):

Appendix C

Julia parameter estimation for analytical model

Julia is used for parameter estimation, the coding used flux machine learning stack in Julia, available on the next page.

Curve fitting using flux in Julia ML

Created by Dany Josué Tomé-Robles in April 7th, 2023

University of South-Eastern Norway

Porsgrunn, April 2023

Changed by Muhammad Muneeb, April 2023

Preliminaries

Loading necessary packages

In [1]:

```
using XLSX, DataFrames, DifferentialEquations, Flux, Optim, ComponentArrays, StatsBase, S
```

```
# Extracting the data from excel sheet
```

In [2]:

```
df = DataFrame(XLSX.readtable("C:/Users/Muneeb/Downloads/Data_sec(1).xlsx", "Data"))
Time = df[:, "Time"] #Time in seconds
ΔS = df[:, "P_pu"]   #Active power in per unit
ΔT_oil = df[:, "Delta_T_oil"]; #Oil Temperature variations "Is not the temperature rise!!
```

In [3]:

```
dataset_ΔT_oil = Array(ΔT_oil);     # Array of oil temperature
```

In [4]:

```
pyplot()

# Create the first plot

p1 = plot(Time, ΔS, label="Active Power loss", xlabel="Time [s]", ylabel="Active Power lo


# Create the second plot with a shared X-axis and a different Y-axis

plot!(twinx(p1),Time, ΔT_oil, label="Oil Temperature",ylabel="Oil Temperature Rise [K]",c
```

Out[4]:

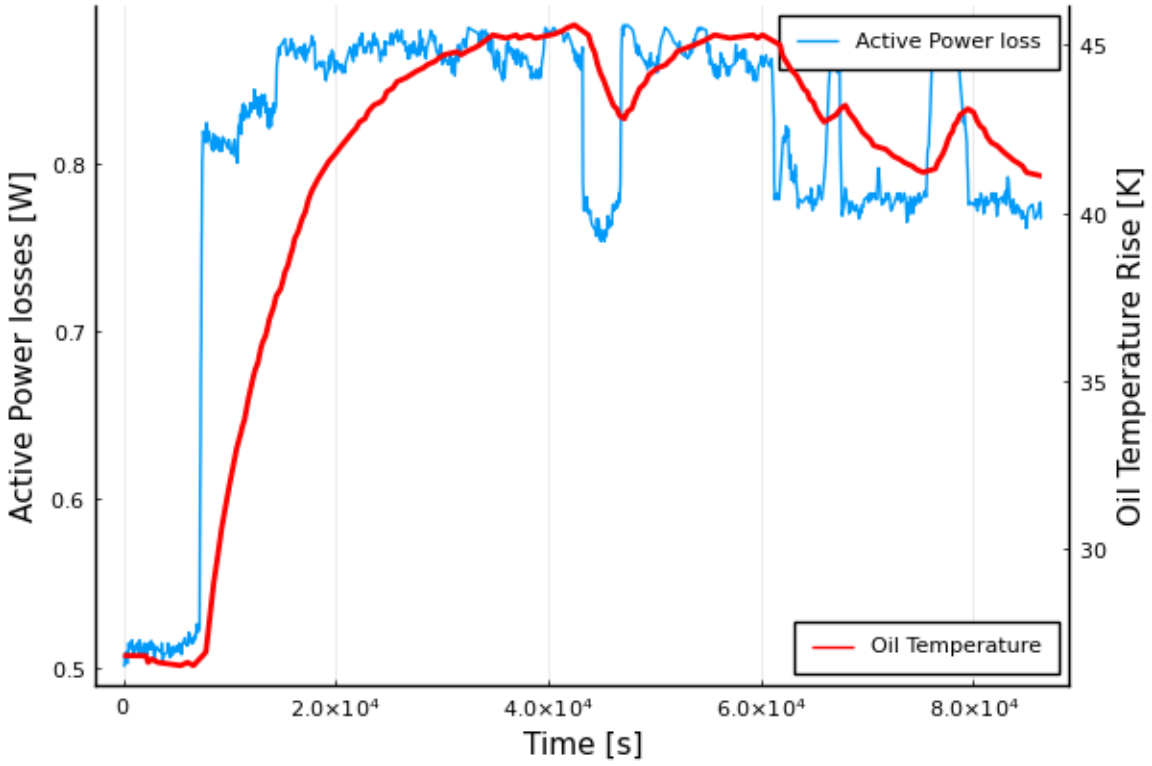

Defining the flux problem

In [11]:

```
# Parameters
Rth_oil = 0.001e-3   # Transformer Oil Thermal Resistance Equivalent [K/W] INITIAL GUESS!


c_oil         = 1.974e3            # Transf. Oil specific heat capacity [J/(kg K)]
m_oil         = 25e3               # Transf. Oil Mass Equivalence [kg]

Cp_oil        = c_oil * m_oil      # Transf. Oil heat capacity [W s/K]

τ_oil         = Cp_oil * Rth_oil #INITIAL GUESS!!!

par = ComponentArray(Rth_oil = Rth_oil, τ_oil = τ_oil)  # Parameter to estimate

p = par

function simple_thermal_Equation(du, u, p, t)
    ΔT_oil = u[1]
    Rth_oil, τ_oil = p.Rth_oil, p.τ_oil
    if t < 1
        ΔS_loss = ΔS[1]
    else
        ΔS_loss = ΔS[Int(round(t))]
    end
    # Transient equation
    du[1] = 1/τ_oil * (ΔS_loss * Rth_oil - ΔT_oil)       # Oil temperature
end

# Training Set
(mean, std) = mean_and_std(ΔT_oil)
training_set = (ΔT_oil .- mean) ./ std

tbegin = 0.0
tend = 1440 * 60
datasize = 1440 * 60
trange = range(tbegin, tend, length=datasize)

tspan = (tbegin, tend)             # Time span to solve for
u0 = [minimum(ΔT_oil)]
prob = ODEProblem(simple_thermal_Equation, u0, tspan, p)

function net()
    Array(solve(prob, Rodas5(), reltol=1e-8, abstol=1e-8, saveat=trange))
end

function loss_func()
    pred = net()
    pred_1 = (pred .- mean) ./ std
    sum(abs2, vec(training_set) .- vec(pred_1))
end

n_epochs = 8000
learning_rate = 1 #Starts with a big learning rate to converge faster since the initial g
data = Iterators.repeated((), n_epochs)
# opt = NADAM()
opt = AdaMax(learning_rate)



# using Plots
```

```
losses = Float64[]

cb = function ()
    loss = loss_func()
    push!(losses, loss)
    display(loss)
end

fparams = Flux.params(p)

Flux.train!(loss_func, fparams, data, opt, cb=cb)
```

```
4.580183582482567e6

4.401075468095357e6

4.227264507135358e6

4.058696176789942 7e6

3.895310575139174e6

3.737043890101826e6

3.5838276802649726e6

3.4355901491636643e6

3.292254659369221e6

3.153741018140137e6

3.019966316345741e6
```

Loss function

In [12]:

```
# 127.37072814535804 losses Muneeb

plotlyjs() #Plotting style PLOTLY
plot(1:length(losses), losses, xlabel="Epoch", ylabel="Loss", legend=false, title="Loss v
ylims!(0,2000)   # set y limits
xlims!(0,length(losses))   # set x limits
```

Out[12]:

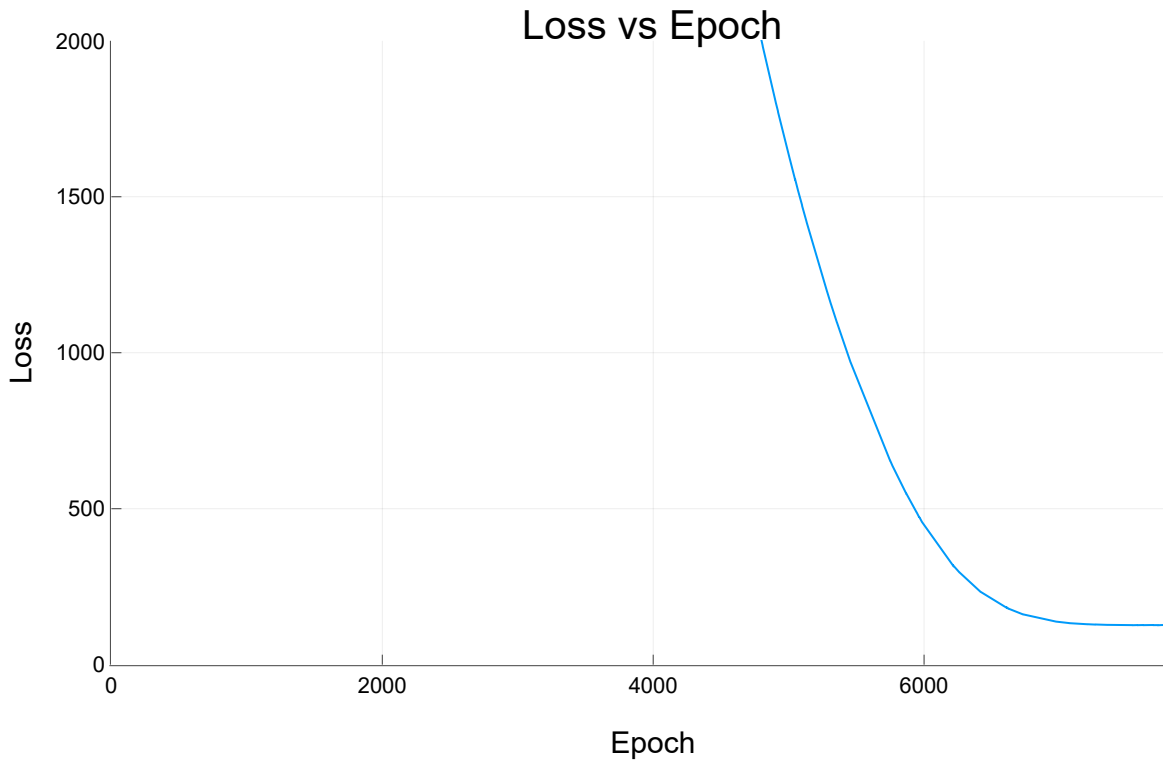

Estimated Parameters

In [13]:

```
Flux.params(p)
```

Out[13]:

```
Params([(Rth_oil = 52.32973167375225, τ_oil = 6716.50688792833)])
```

In [14]:

```
p.Rth_oil/118e6, p.τ_oil/60
```

Out[14]:

```
(4.434723023199343e-7, 111.94178146547216)
```

Initial Parameter (Guess)

In [15]:

```
Rth_oil/118e6, τ_oil/60
```

Out[15]:

```
(8.474576271186441e-15, 0.8224999999999999)
```

Thermal Model Approximation

In [16]:

```
sol = solve(prob,Rodas5(),reltol=1e-10,abstol=1e-8, saveat=trange);
plotlyjs() # It is use to be able to change angles and zooming of the plots
# pyplot()
plot(Time,ΔT_oil, xlabel="Epoch", ylabel="Loss",label="Transformer Data")
plot!(sol,label="Thermal Equation Approximation",title="Simple Model Approximation",leger
```

Out[16]:

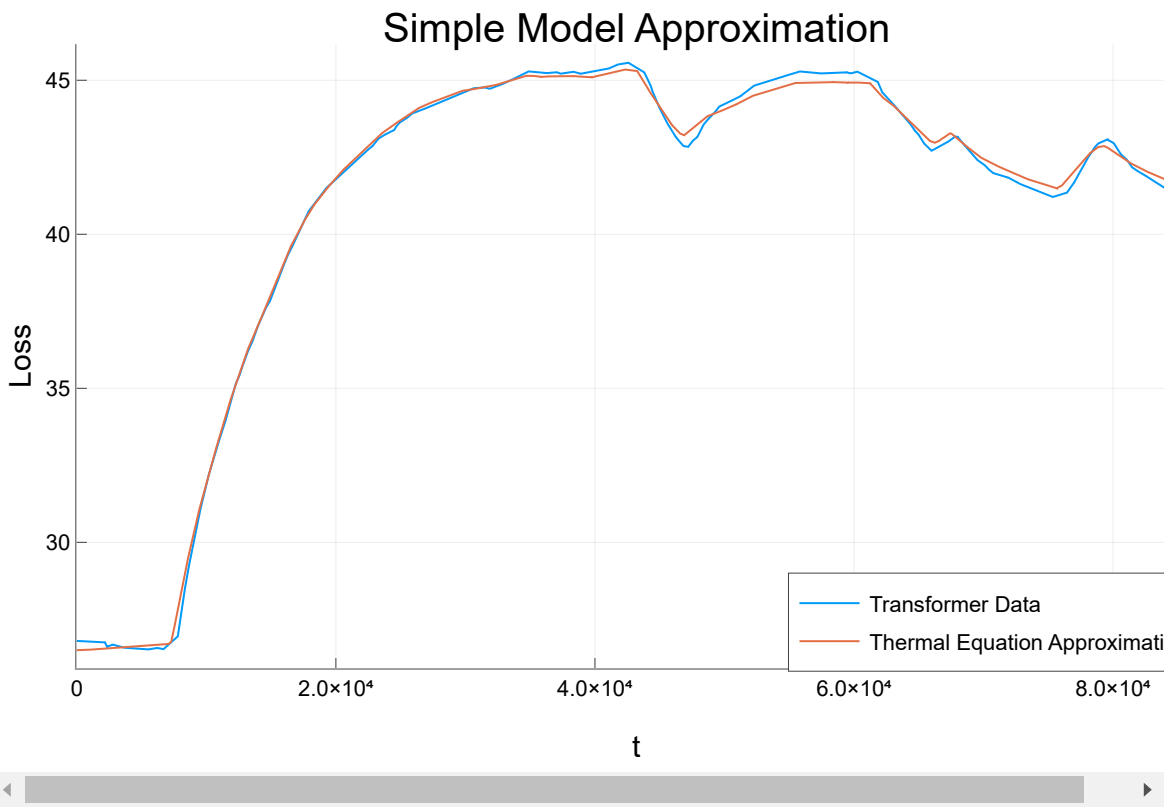

In [ ]:

In [ ]: